Near-Surface Volcanic Rocks in the Southeastern Nechako Basin, South-Central British Columbia (Parts of NTS 092N, O, 093B, C): Interpretation of the Canadian Hunter Seismic Reflection Surveys and First-Arrival Tomographic Inversion

N. Hayward, Department of Earth Sciences, Simon Fraser University, Burnaby, BC, nhayward@nrcan.gc.ca

A.J. Calvert, Department of Earth Sciences, Simon Fraser University, Burnaby, BC

Hayward, N. and Calvert, A.J. (2010): Near-surface volcanic rocks in the southeastern Nechako Basin, south-central British Columbia (parts of NTS 092N, O, 093B, C): interpretation of the Canadian Hunter seismic reflection surveys and first-arrival tomographic inversion; *in* Geoscience BC Summary of Activities 2009, Geoscience BC, Report 2010-1, p. 203–226.

Introduction

Renewed interest in the Nechako Basin has been a result of development of the region's mineral resources following the impacts of pine beetle infestation on the region's forestry industry. Although forestry road access into the region is good, there are a number of impediments to interpretation of the basin's stratigraphy and structure, and to the evaluation of its hydrocarbon and mineral potential. These include the extensive vegetation and surficial deposits, the limited outcrop of Jura-Cretaceous rocks, and the sparsity and variable quality of seismic reflection data. In this paper, the geology and structure of near-surface rocks are investigated using first-arrival tomographic-inversion velocity models.

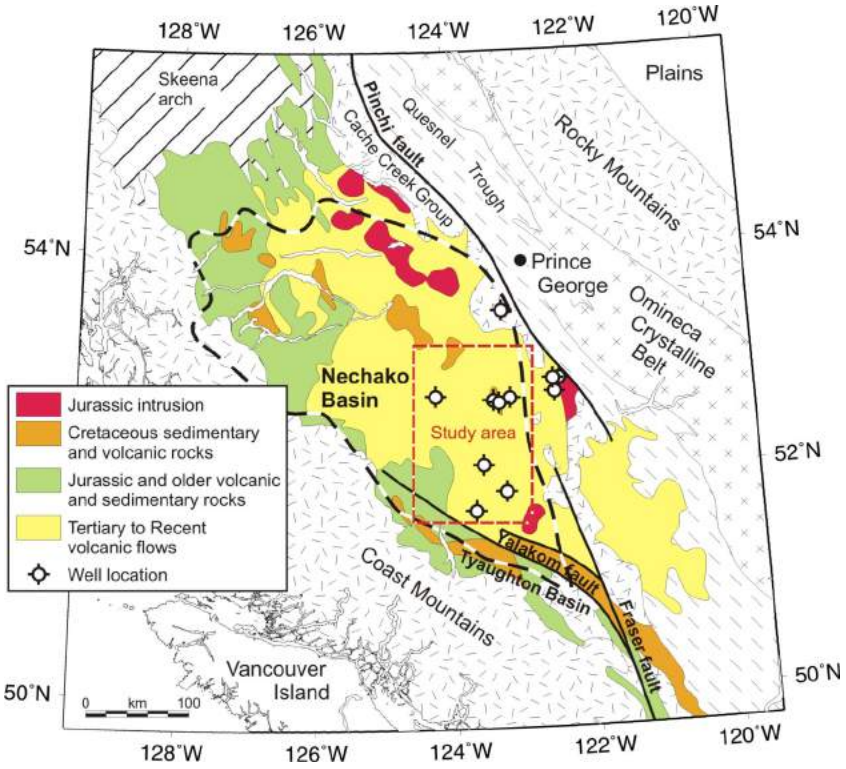

Figure 1. Location of the Nechako Basin and simplified geology of its western Canadian Cordillera setting (modified from Hayward and Calvert; 2009b). Black and white dashed box shows the study area (Figure 2).

The Nechako Basin is primarily a Jurassic to Oligocene successor basin located in the interior plateau of south-central British Columbia (Figure 1), between the Rocky Mountains and Coast Mountains (Hickson, 1990). The basin is bounded by the Coast Mountains and the Yalakom fault to the west, the Fraser fault to the east, the Cretaceous Skeena Arch to the north and the Jura-Cretaceous Tyaughton Basin to the south.

The basin formed in part from and following accretion of the terranes of the western Canadian Cordillera, where the oceanic Cache Creek Terrane separates surface exposures of the Stikine and Quesnel volcanic arc terranes (Struik and MacIntyre, 2001). Westward-directed thrusting occurred during basin initiation prior to 165 Ma (Schiarizza and MacIntyre, 1999) at the boundary between the Stikine and Cache Creek terranes, and transpressional tectonic processes were dominant until the Eocene. The primary Yalakom and Fraser faults are associated with this Eocene shift to a dextral transtensional regime (Price, 1994), which was accompanied by regional volcanism. These Eocene volcanic rocks, which blanket the Jura-Cretaceous sedimentary basin, were later overlain by a varying thickness of Neogene volcanic rocks and Quaternary glacial and drift deposits.

Keywords: *Nechako Basin, tomography, potential field, physical properties*

This publication is also available, free of charge, as colour digital files in Adobe Acrobat® PDF format from the Geoscience BC website: http://www.geosciencebc.com/s/DataReleases.asp.

Summary of Basin Stratigraphy and Structure

Seismic reflection profiles acquired by Canadian Hunter Exploration Limited (Canadian Hunter) in the 1980s were recovered and reprocessed in 2006 by Arcis Corporation.[1] These data formed the basis for the re-examination of the subsurface structure and stratigraphy of the southeastern Nechako Basin by Hayward and Calvert (2008b). Regional interpretation of the seismic reflection data was divided into four blocks based on seismic data location and variations in geological structure and stratigraphy (Figure 2):

1) Block A (southern Redstone area), in the southern part of the study area, is centred on the Canadian Hunter Redstone wells d-94-G and b-82-C, and seismic lines 160-01 to -19.

2) Block B (western Redstone area), centrally located, includes the single seismic line 160-17, which intersects Hudson's Bay well c-75-A. The single crooked seismic line in this block could not be modelled by the two-dimensional (2-D) tomographic methods used here.

3) Block C (Chilcotin area), in the northwestern part of the study area, contains the Canadian Hunter Chilcotin well b-22-K and seismic lines 161-01 to -09.

[1] *These seismic data are currently confidential, but can be obtained for noncommercial purposes through Geoscience BC with a specific research agreement.*

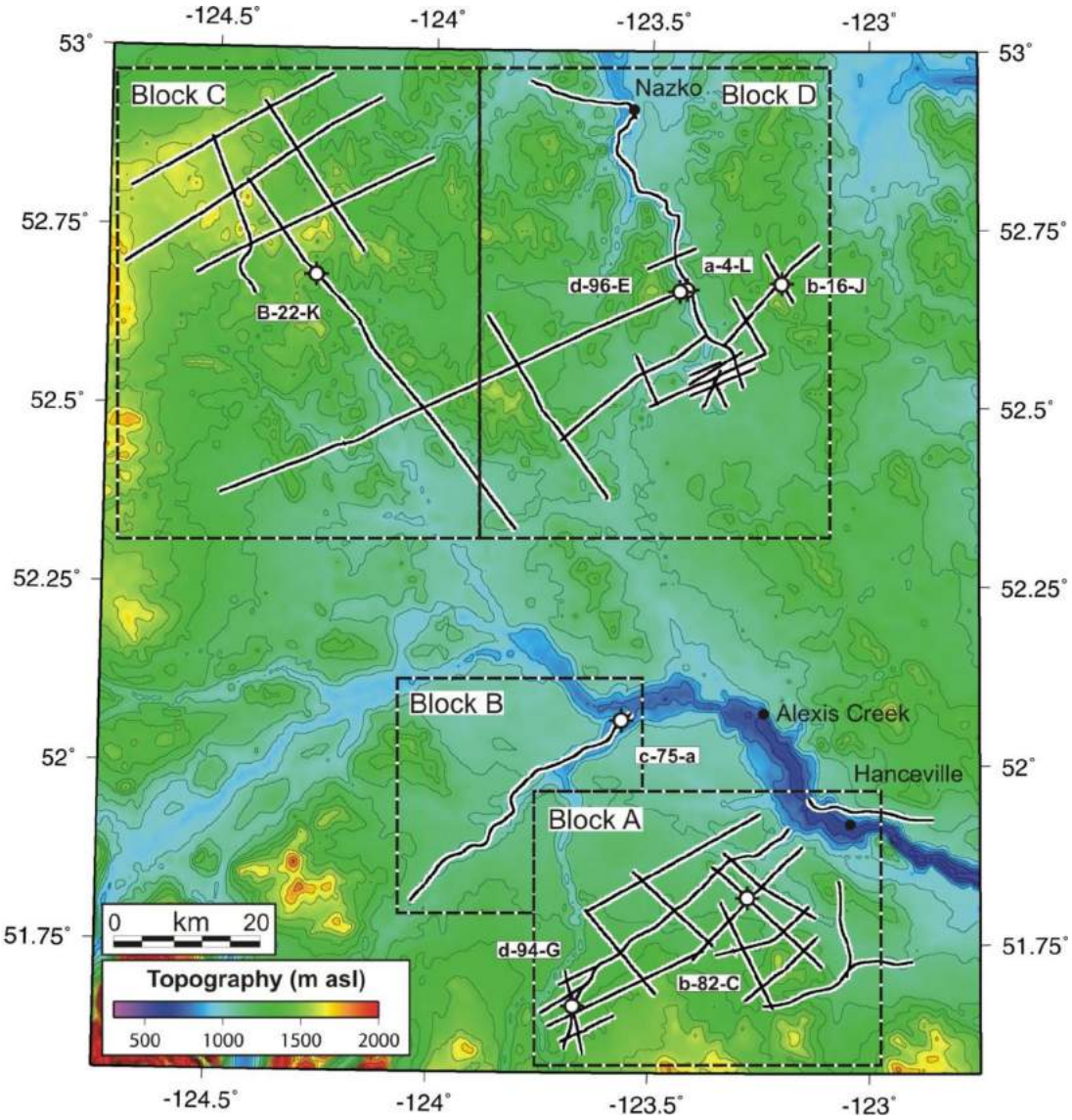

Figure 2. Location of Canadian Hunter seismic reflection lines (white bordered black lines) and topography of the study region, southeastern Nechako Basin, south-central British Columbia. Contour interval 100 m. Large dashed boxes show the original study blocks (A, B, C and D). Black circles show well locations.

4) Block D (Nazko area), in the northeastern part of the study area, includes wells Honolulu Nazko a-4-L, Canadian Hunter Nazko d-96-E and Canadian Hunter–Esso Nazko b-16-J, and seismic lines 159-01 to -15 and 162-02.

The southeastern Nechako Basin consists of remnants of Cretaceous fold-and-thrust belts that have been segmented during roughly north-northwest-trending Eocene dextral transtension associated with the Fraser and Yalakom faults (Figure 3). Jura-Cretaceous rocks that remain in the basin are interspersed with volcanic and intrusive basement highs and Eocene pull-apart basins that host volcaniclastic deposits. Seismic interpretation of the Cretaceous thrust faults suggests roughly east-west convergence, which is generally in agreement (Rusmore et al., 2000) with the mid-Cretaceous contractional event that was responsible for the formation of the northeast-verging Waddington thrust belt (Rusmore and Woodsworth, 1991).

In block A (Figure 3), Cretaceous compressional structures were reactivated under Eocene dextral transtension. A sub-basin in the vicinity of well d-94-G contains Cretaceous rocks of the Taylor Creek Group, which overlie volcanic rocks of the Cretaceous Spences Bridge Group. Rocks of the sub-basin form a northwest-plunging faulted anticline, which shows evidence of northwest-southeast Eocene strike-slip deformation. A low-angle, southwest-dipping detachment divides these rocks from shallow basement to the northeast. Another sub-basin, adjacent to well b-82-C, is more poorly deformed. Faulting is concentrated at the northwest (thrusting) and southeast (strike-slip) margins, which are marked by basement and Bouguer gravity highs (Figure 3b).

The block C region is dominated by a north-northeast-trending extensional basin that contains more than 4 km of Eocene volcaniclastic and sedimentary rocks (Riddell et al., 2007). Faults bounding and within the basin have strikes that echo the two dominant trends (northwest and north-northeast) observed in the potential field anomalies (Figure 3b). The basin was likely formed during Eocene dextral transtension, with internal basin folding and faulting occurring late in its history.

In the block D region, sedimentary rocks of the Taylor Creek Group, thrust eastwards during the Cretaceous, were subsequently deformed and truncated by strike-slip faults during Eocene dextral transtension. Strike-slip faults in southwestern block D (trend similar to the Yalakom fault system) and eastern block D (trend similar to the Fraser fault system) may form an extensional right-stepping system along an east-west discontinuity that divides the Eocene strike-slip faults in southwestern block D from Cretaceous thrust faults in northwestern block D.

Near-Surface Rocks in the Southeastern Nechako Basin

Geological mapping in the southeastern Nechako Basin (e.g., Riddell, 2006) has broadly constrained the areal extent of the volcanic units that overlie the Jura-Cretaceous rocks (Figure 4a); however, detailed interpretation is limited by lack of observable relationships. The low density of surface exposures precludes a full understanding of the extent, thickness and variations in lithology of the volcanic rocks below the widespread overburden (be it Quaternary deposits or volcanic rocks younger than the age of the rocks of interest). Interpretations of near-surface stratigraphy derived from oil exploration wells (Figure 5) do not always match surface geological maps. Regionally incomplete mineralogical descriptions and limited geochronology may also lead to incorrect identification (Haskin et al., 1998) of the volcanic rocks of the Neogene Chilcotin Group (28–1 Ma; Anderson et al., 2001), and the Eocene Endako Group (ca. 51–45 Ma) and Ootsa Lake Group (ca. 53–48 Ma) in the field.

Seismic reflection data gave very poor images of the near surface, irrespective of lithology. Therefore, seismic velocity estimated from the tomographic inversion of first arrivals from these seismic reflection data can provide a valuable additional constraint on the distribution and thickness of the near-surface Eocene and Neogene volcanic rocks (Hayward and Calvert, 2009a). All relevant geological and geophysical information, including wells (drilled by Canadian Hunter Exploration Limited, Esso, Honolulu Oil Corporation Limited and Hudson's Bay Oil and Gas Company Limited) and geological maps (e.g., Riddell, 2006) guided the interpretation. Primary stratigraphic control is provided by well data (Riddell et al., 2007), and surface geological maps (e.g., Riddell, 2006) aided in the classification of the near-surface stratigraphy.

The Chilcotin Group has been locally interpreted to include a diverse range of lithofacies, including the Chasm (Mathews, 1989; Farrell et al., 2007), Bull Canyon (Gordee et al., 2007) and Dog Creek (Farrell et al., 2007). The Chilcotin Group consists primarily of flat to shallow-dipping basaltic flows, which are columnar jointed or massive with some hyaloclastite, tephra and pillow basalt, and weathered paleosols (Riddell, 2006; Andrews and Russell, 2007).

Volcanic rocks of the Eocene Endako and Ootsa Lake groups have undergone limited local study. Geological mapping (Riddell, 2006) showed that the Endako Group consists of vesicular and amygdaloidal basaltic to andesitic flows with tuff, breccia, and minor sedimentary rocks. The Ootsa Lake Group is characterized by intermediate to felsic flows, accompanied by tuff, breccia and sedimentary rocks. In the vicinity of Fort Fraser and Burns Lake (54°N, 125°W), to the north of the current study area, the Endako

and Ootsa Lake groups have been dated at ca. 51–45 Ma and ca. 53–48 Ma, respectively (Grainger et al., 2001).

Cretaceous sedimentary rocks, which include sandstone, conglomerate and minor volcaniclastic rocks, outcrop (Figure 4b) in central block D (Taylor Creek Group) and southwestern block A (Taseko River strata; Riddell, 2006). The Cretaceous Spences Bridge Group outcrops in southwestern block A (Figure 4b), around well d-94-G, and comprises volcanic flows, breccia and tuff, with volcanic siltstone to conglomerate (Riddell, 2006). Jurassic or Cretaceous granodioritic intrusions are found in contact with the Spences Bridge Group in block A and in southwestern block C.

First-Arrival Tomographic Inversion (2-D)

Seismic waves propagate laterally through the near surface and are recorded by geophones deployed along the seismic line. The arrival times of these waves at different source-receiver offsets provide an indication of the speed of propagation through the subsurface (i.e., seismic velocity). First-arrival traveltimes are usually the most accurately determined because there are no interfering secondary arrivals. First arrivals form the basis for a class of seismic tomographic methods that derive the vertical and lateral variation in seismic P-wave velocity (e.g., Aldridge and Oldenburg, 1993; Zelt and Barton, 1998). The depth of investigation is limited by the maximum source-receiver offset and the vertical velocity gradient; seismic waves propa-

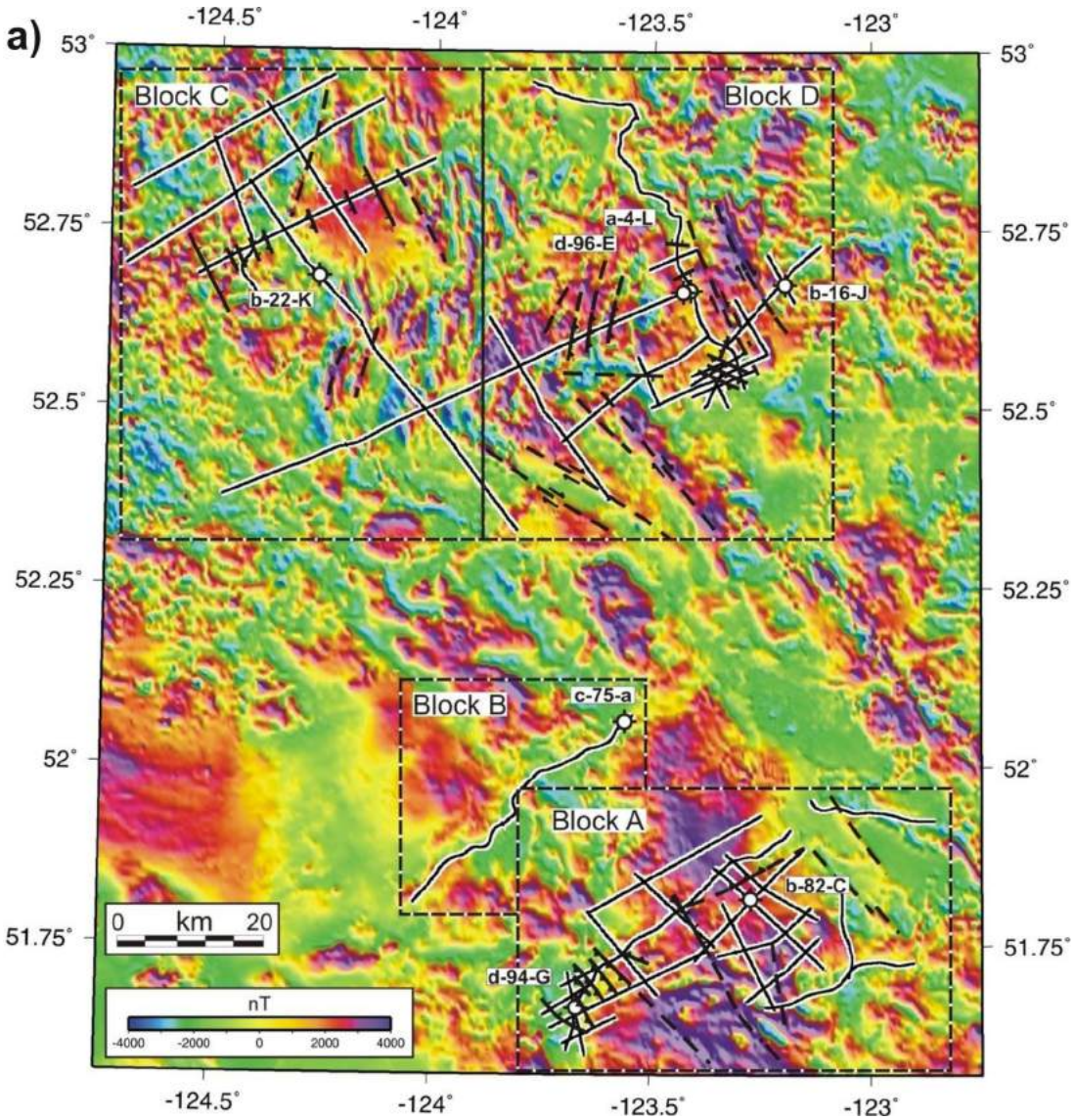

Figure 3: Summary of the structure of the southeastern Nechako Basin, south-central British Columbia: **a)** magnetic anomalies, **b)** [**facing page]** Bouguer (2.30 g/cm^3) gravity anomalies. Canadian Hunter seismic reflection lines shown by white bordered black lines. Large dashed boxes show the modified study blocks (A, C and D). Black circles show well locations.

gate preferentially through the upper part of low-gradient layers.

First-arrival tomographic inversion methods have been used effectively to investigate the geological structure and near-surface velocity. For example, tomographic models have revealed along-strike variation in the structure of the Devil's Mountain fault (Hayward et al., 2006) and the Seattle fault zone (Calvert et al., 2003) in Washington. Hayward and Calvert (2007) used similar methodology to constrain the seismo-stratigraphy of the Tofino Basin, offshore Western Canada. Schmid et al. (2001) used similar techniques to show the velocity structure across the Tan-Lu fault in the easternmost Dabie Shan, China.

In the southeastern Nechako Basin (Hayward and Calvert, 2008a), preliminary results showed that these velocity models can reveal both vertical and lateral near-surface stratigraphic variation in rocks that are otherwise poorly imaged by seismic reflection profiles. Seismic reflection images are often poor in areas where Chilcotin and/or Endako and Ootsa Lake Group rocks outcrop, especially to the northwest (block C, Figure 4b). However, the lack of a clear relationship between surface lithology and seismic image quality (Figure 6) suggests significant variations in the thickness, physical properties and structure of the surface volcanic rocks.

Canadian Hunter Seismic Reflection Data

The seismic reflection data used in this study were acquired along cutlines by Canadian Hunter Exploration Limited in the early 1980s. A vibroseis source (five 16,000 lb. Failing vibes over 100 m) gave a 15 s sweep over a frequency of 10–70 Hz (linear). The shot interval was 100 m except for lines CH159-02, -02A, -11, -12, -13, -14 and -15, which had an interval of 50 m (Figure 4b). A split-spread array with 96 or 48 (lines CH159-02 and -02A) channels, with in-

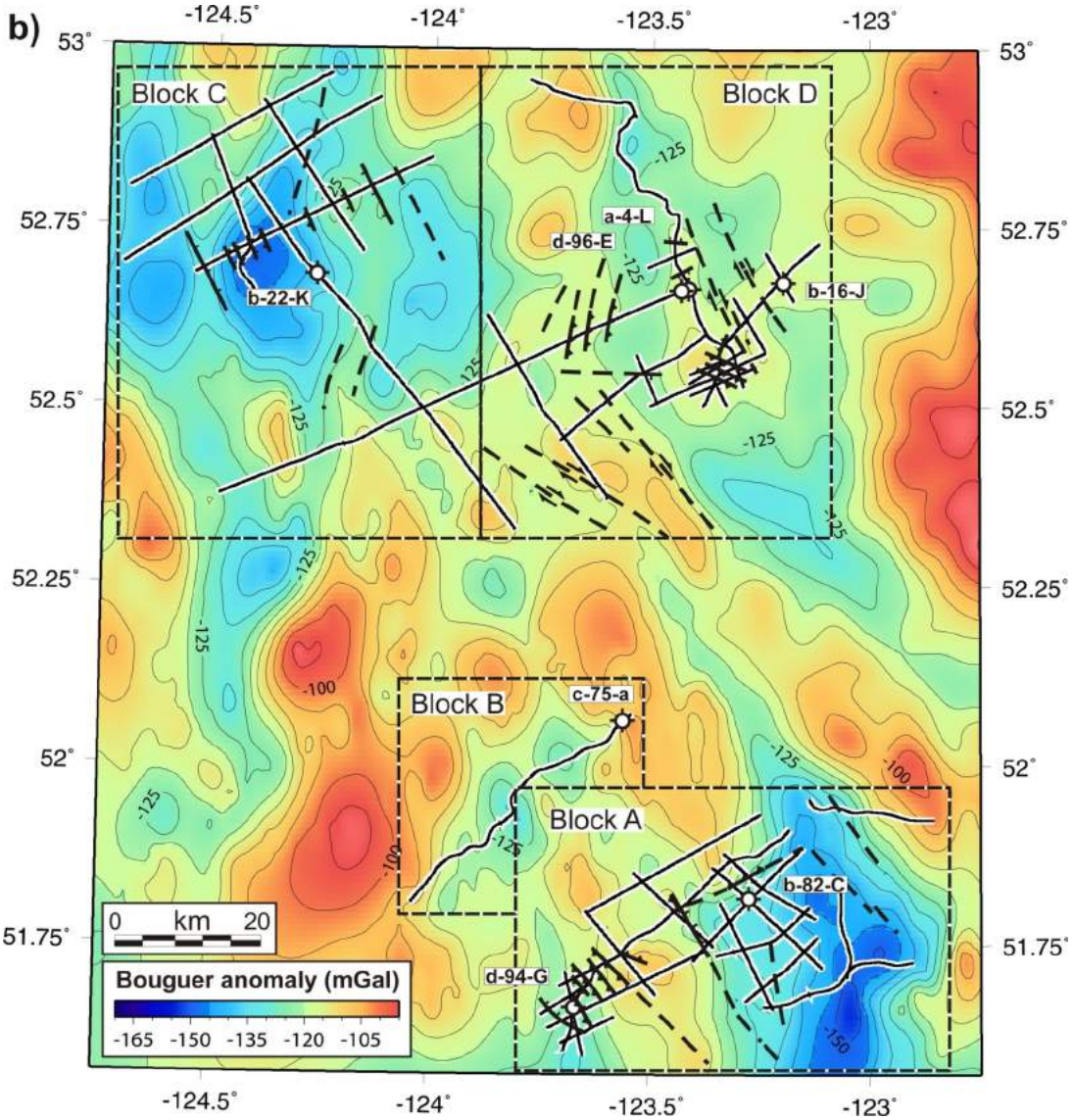

dividual receiver groups 100 m long, consisted of L-15 geophones (frequency of 8 Hz) centred every 50 m. The maximum source-receiver offset was 2550 m, except for lines CH159-02 and -02A, where it was 1350 m. Four seconds of data were recorded at a sample interval of 4 ms.

Tomographic Inversion Method (2-D)

First arrivals (the direct wave and subsurface refractions) are clearly identified on most shot gathers to the farthest offset. The first-arrival traveltimes picked during seismic reflection reprocessing by Arcis in 2006 were manually edited (Figure 7) in ProMAX™ software (Landmark Graphics Corporation) to eliminate pick errors and improve pick accuracy (±25 ms). Pronto software (Aldridge and Oldenburg, 1993) was used to invert these traveltimes for seismic P-wave velocity for all (total of ~790 km) straight seismic profiles (Figure 4b). A finite-difference solution to the eikonal equation was used to derive first-arrival times to all locations in a subsurface velocity grid (25 m grid spacing). Ray paths from source to receiver were created through the traveltime grid, along the steepest descent direction.

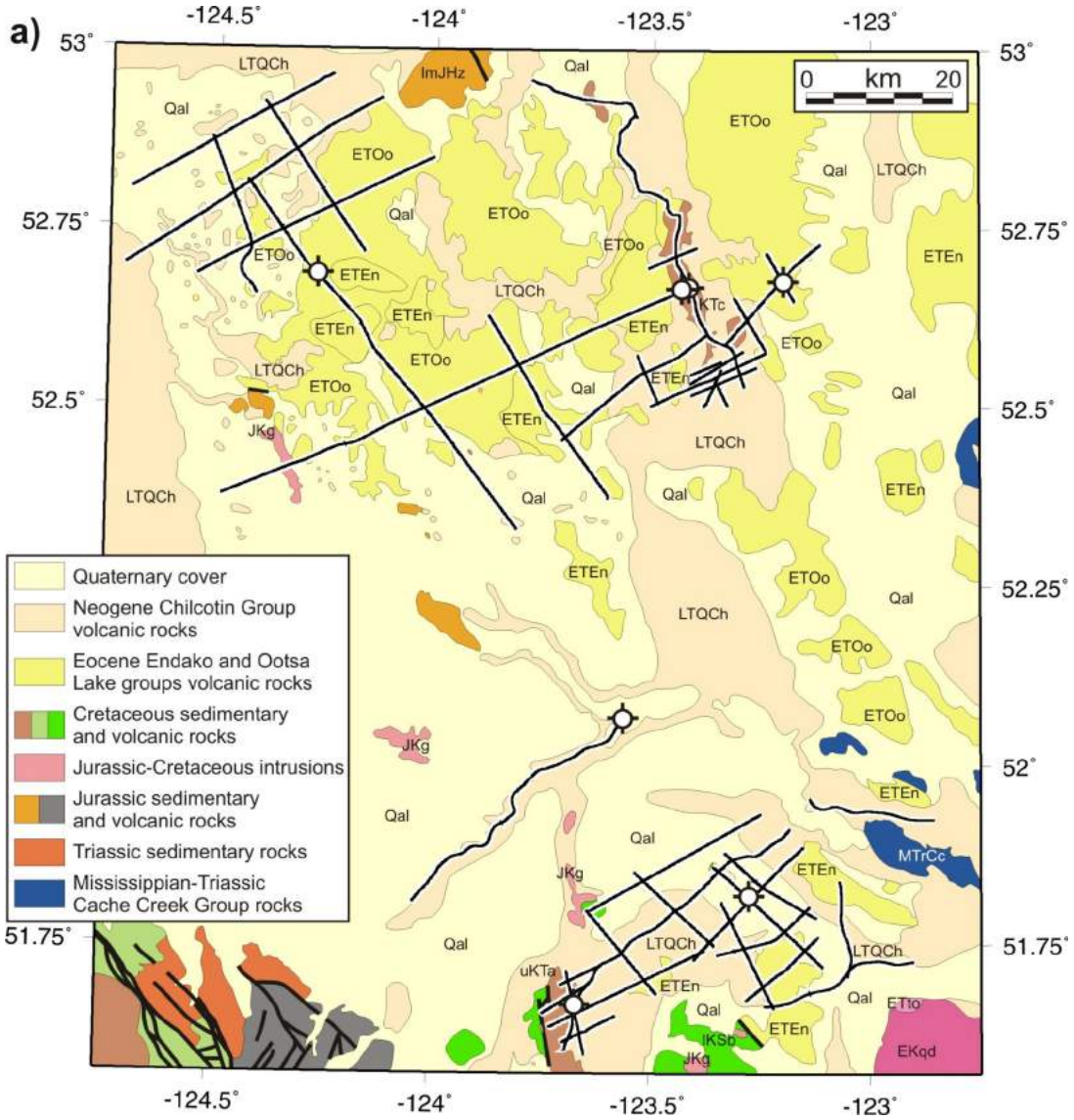

Figure 4: Geology of the study area (modified from Riddell, 2006), southeastern Nechako Basin, south-central British Columbia, showing: **a)** location of seismic reflection profiles (white bordered black lines); and **b) [facing page]** location of presented first-arrival tomographic models (heavy black lines), with heavy dotted lines showing presented corrugation models, large dashed boxes showing the modified study blocks (A, C and D) and boxed text showing seismic line numbers and wells. Abbreviations: ETEn, Eocene Endako Group; ETOo, Eocene Ootsa Lake Group; ETto, Eocene tonalite; LTQCh, Neogene Chilcotin Group; KTc, Cretaceous Taylor Creek Group; EKqd, Cretaceous quartz diorite; uKTa, Taseko River strata; lKSb, Cretaceous Spences Bridge Group; Qal, Quaternary deposits; lmJHz, Jurassic Hazleton Group; JKg, Jura-Cretaceous granodiorite.

In order to obtain a realistic final model, a starting model is required that closely matches the true P-wave velocity. Available sonic logs from six wells (Figure 5) guided the selection of starting-model parameters. However, near-surface sonic data are often absent and well logs are only representative of point locations in a region where velocity is highly variable. The chosen 1-D starting model was estimated from a few trial inversions with a magnitude and gradient that is overall similar to the well sonic logs (Figure 5). Increasing the magnitude of the velocity in the starting model results in unrealistic near-surface velocity gradients. For example, an increase in surface velocity of the starting model for line CH160-05 to 4000 m/s (with a gradient of 1.5 s^{-1}) results in a negative velocity gradient of ~25 s^{-1} and a decrease of ~400 m/s in the upper ~30 m of the model, rather than a smooth increase in velocity with depth. Therefore, following evaluation of the results of a range of starting-model parameters, the surface velocity of the starting model (Figure 5) for all lines was set to 3500 m/s (gradient of 1.5 s^{-1}), for model consistency and smoothness.

A perturbation in the velocity model was calculated from the difference between the calculated and observed first-arrival traveltimes for each of 15 iterations to give each final velocity model. The models show a combined reduction in traveltime misfit (e.g., Figures 8a, b) from a mean RMS error of 70.6 ms to 20.6 ms. The velocity and ray data were smoothed for display using a continuous-curvature gridding algorithm (Smith and Wessel, 1990) at a grid spacing of 5 m.

Maximum ray penetration is controlled primarily by the maximum source-receiver offset (2550 or 1350 m) and subsurface geology. The highest density of rays typically gave a well-constrained estimate of the P-wave velocity for depths of up to ~450 m, although ray penetration some-

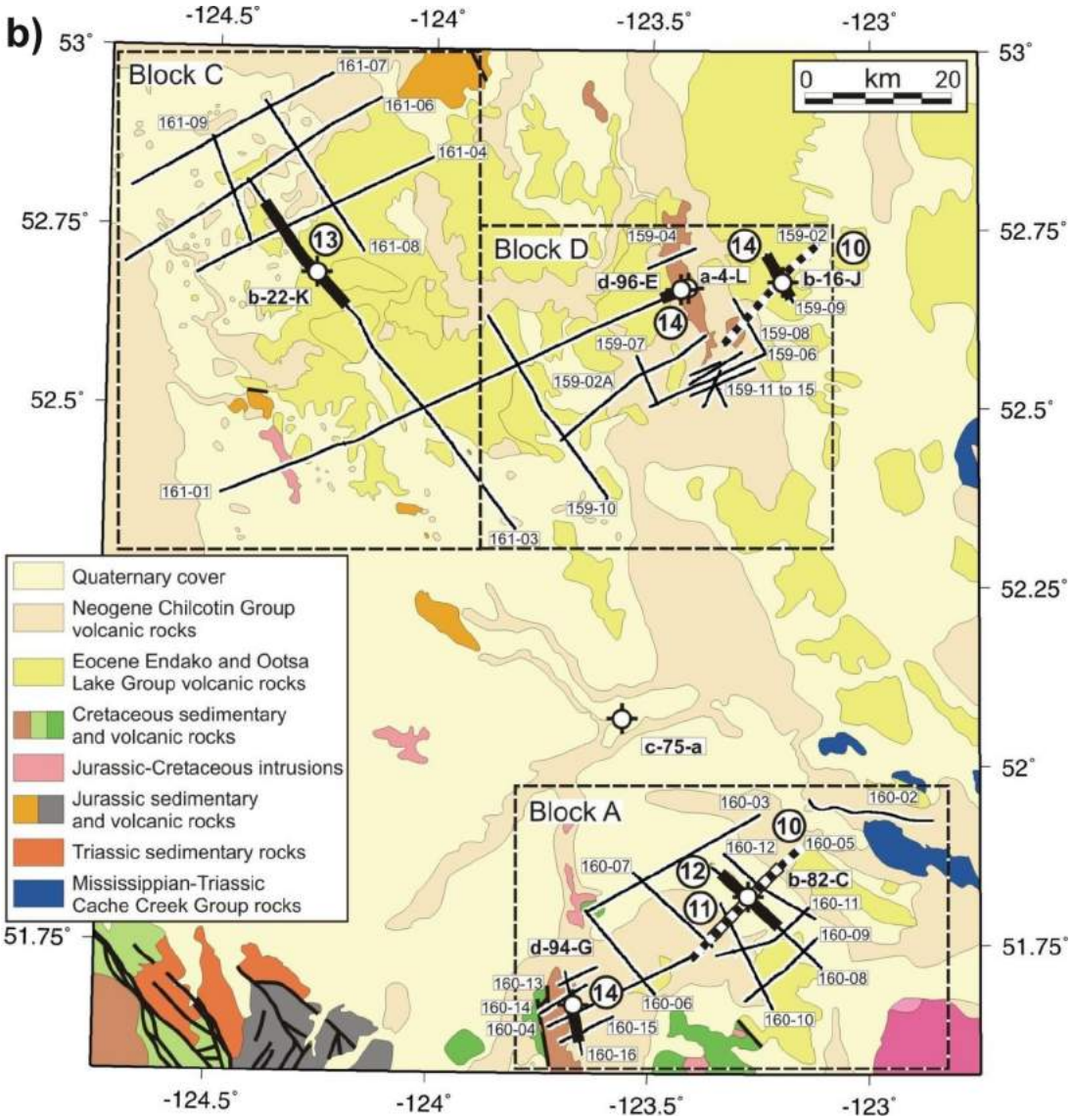

times locally reached ~700 m. The lower maximum offset of 1350 m for two seismic lines (CH-159-02 and -02A) resulted in a significantly reduced depth of maximum ray penetration. Here, estimates of P-wave velocity are best constrained for depths of up to ~100 m, but locally up to ~500 m.

Reliability of the Velocity Model Estimates

The reliability of the velocity models was assessed by comparing the mean velocity in the upper 175 m between the final (starting model surface velocity 3500 m/s with a 1.5 s^{-1} gradient) and alternative models, using starting models with a lower surface velocity (2500 and 3000 m/s). For seismic reflection line CH160-05, the model derived from a starting model with a surface velocity of 3000 m/s (1.5 s^{-1} gradient) gave velocities 20 m/s higher to 70 m/s lower (mean 14.02, standard deviation 17.18) than the final model. The model derived using a starting model with a surface velocity of 2500 m/s (1.5 s^{-1} gradient) gave a model with velocities 30 m/s higher to 140 m/s lower (mean 29.01, standard deviation 34.83) than the final model. Despite the 500–1000 m/s reduction in the starting-model velocity, the result is robust, with a mean velocity that varies only by a maximum of 4% of the final model in the upper 175 m.

Velocity Model Resolution

Corrugation tests were used to assess the ability of the tomographic velocity models in the Nechako Basin to accurately reflect lateral variations in velocity and structure across the modelled depth range. Corrugation tests for lines

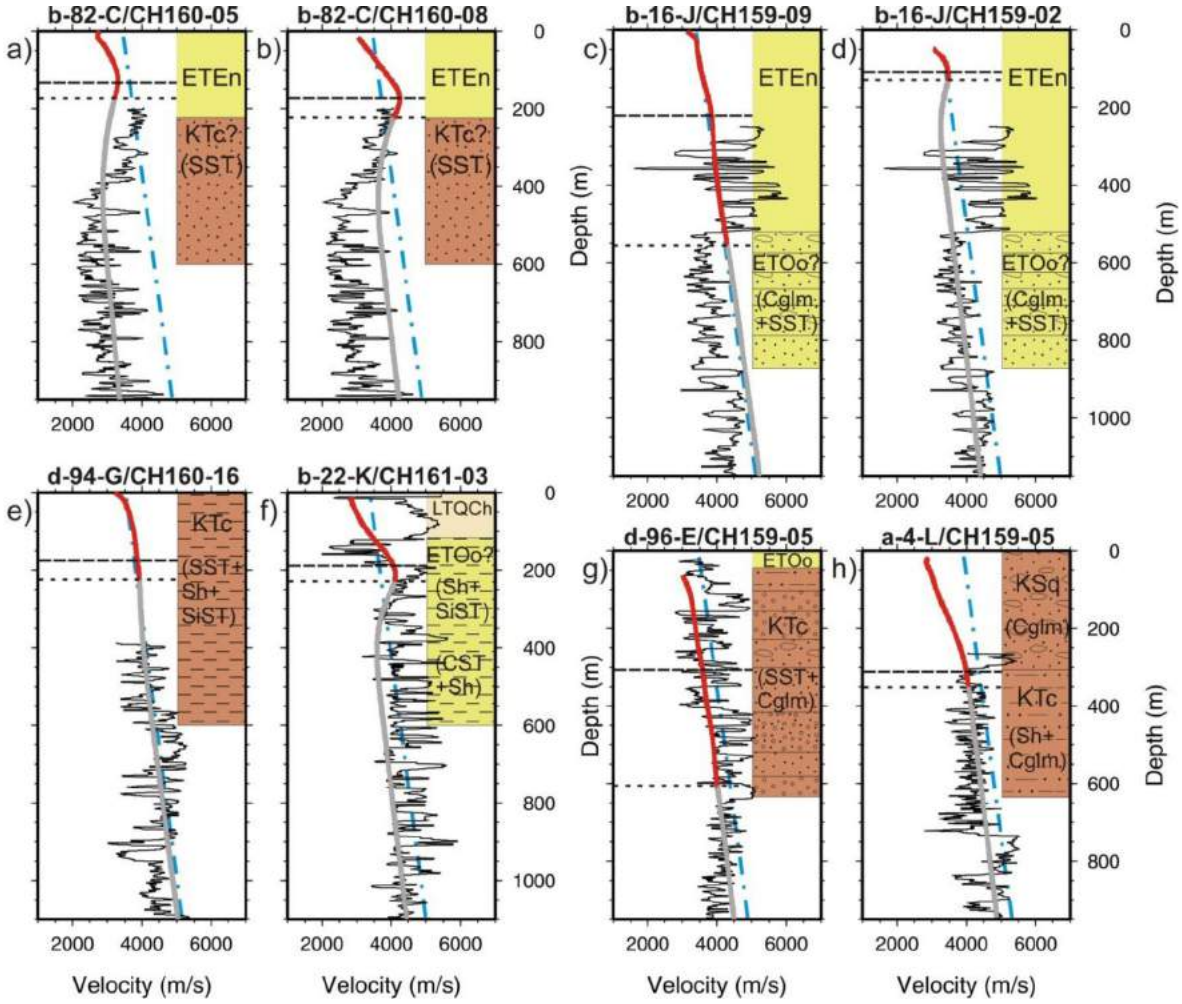

Figure 5: Comparison of tomographic velocity models (heavy red/grey lines) with well sonic logs (thin solid black lines) and stratigraphy (Ferri and Riddell, 2006), southeastern Nechako Basin, south-central British Columbia. Abbreviations: ETEn, Endako Group; ETOo, Ootsa Lake Group; LTQCh, Chilcotin Group; KTc, Taylor Creek Group; KSq, Silverquick Group. Rock types: Cglm, conglomerate; SST, sandstone; SiST, siltstone; CST, claystone; Sh, shale. Heavy red lines show constrained model and heavy grey lines show unconstrained model. Thin solid black lines show the well sonic log (manually de-spiked, and filtered with a four-point (~60 cm) median filter). Pale blue dot-dashed line shows the starting velocity model. Horizontal dashed line shows the depth of maximum ray density at the well. Horizontal dotted line shows the base of the velocity model (base of ray coverage) at the well. Depth is relative to the topography at the well. Non-coincidence of the top of the velocity model and the well top is due to topography and projection of the well onto the model profile.

CH160-05 and CH159-02, with maximum offsets of 2550 and 1350 m respectively, are shown in Figures 9a and b. For each test, vertical corrugations with constant widths (0.25, 0.5 and 1.0 km), depths from the ground surface to the base of the model, and a variation in the slowness of ±10% velocity variation were added to the final velocity model to create three independent tests for each line. The predicted traveltimes calculated through the perturbed models were used to create a corrugation velocity model with the final velocity model as the starting model. When the final velocity model is subtracted from the corrugation velocity model, the regenerated corrugations shown in Figure 9 remain.

The corrugation tests show that the ability to resolve velocity anomalies at depth increases with anomaly width. Anomalies with a width of 1.0 km are well resolved above a depth of ~300 m, or the maximum depth of ray penetration if shallower. Anomalies of 0.5 km width are resolved above a depth of ~250 m and those of 0.25 km width are only resolved in the near surface. Lines with a maximum offset of 1350 m (CH-159-02 and -02A) show no reduction in resolution, despite the reduced depth of maximum ray penetration.

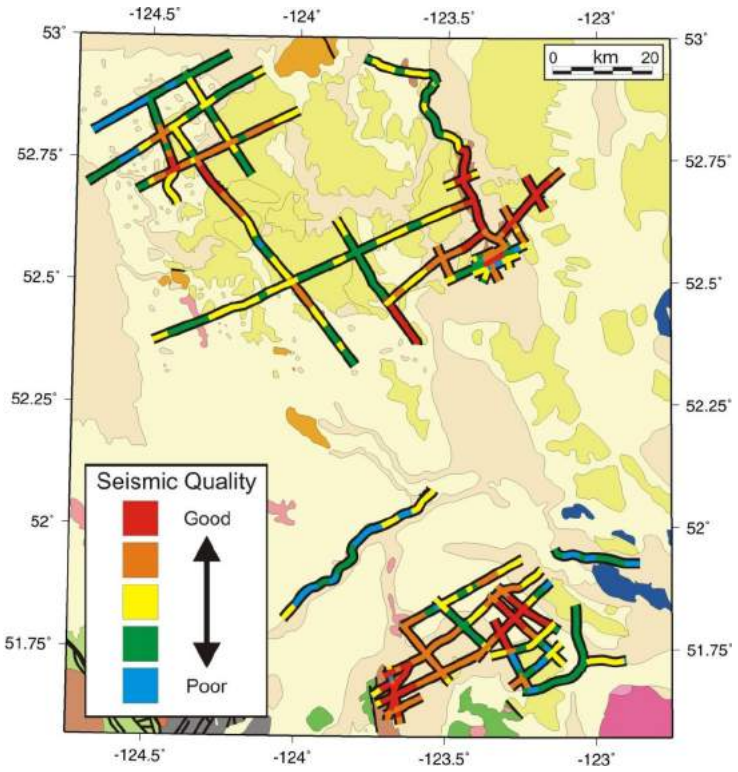

Figure 6: Seismic reflection data quality overlain on surface geology (Riddell, 2006) of the southeastern Nechako Basin, south-central British Columbia. Legend: blue, no coherent reflections; green, reflections that are slightly coherent over short distances; yellow, some coherent reflections, laterally continuous over short distances; orange, coherent reflections to a two-way travetime (TWTT) of ~1 s, laterally continuous over short to medium distances; red, coherent reflections to a TWTT of >1 s, laterally continuous over short to medium distances.

Near-Surface Velocity Character of the Southeastern Nechako Basin

Comparison of Velocity Models with Well Sonic Logs and Lithology

Subsurface lithological information where the surface geology is often obscured by vegetation or Quaternary deposits is provided by six wells (Figure 5) that intersect the modelled seismic reflection lines. Most of the wells penetrated the volcanic rocks, which dominate the surface geology, the thicknesses of which are shown in Table 1. Well lithology may be referenced to the velocity models and available well sonic logs for the analysis of the region's velocity character.

In well b-82-C (Figures 5a, b), ~221 m of the Endako Group volcanic rocks overlie Cretaceous sandstone (Ferri and Riddell, 2006). Velocity models CH160-05 (Figure 10b) and CH160-08 (Figure 11b) have a high density of rays (Figures 10a, 11a) that focus just above the base of the Endako Group (at ~170 m and ~220 m, respectively). The interval of the Endako Group estimated by the tomographic model has a velocity of ~2600–4250 m/s at well b-82-C.

At the top of well b-22-K (Figure 5f), ~116 m of Chilcotin Group basaltic rocks are interpreted (Ferri and Riddell, 2006) to overlie 477 m of shale, siltstone and minor volcanic rocks, possibly of the Ootsa Lake Group (Riddell et al., 2007). Adjacent to the well (Figure 4b), however, geological maps show volcanic rocks of the Ootsa Lake Group. Velocity models (Figures 5f, 12b) show a good correspondence with the sonic log velocity of the upper part of the sedimentary section, but underestimate that of the Chilcotin Group. A sharp increase (~1500 m/s) in the sonic velocity at a depth of ~180 m is coincident with the peak of ray density (Figures 12a and 5f).

Approximately 517 m of Eocene Endako volcanic rocks, which overlie sedimentary rocks of Paleocene to possibly Eocene age (Ferri and Riddell 2006), were intersected by well b-16-J (Figure 5c). The highest density of rays (Figure 13a) for velocity model CH159-09 is in the upper ~220 m, where sonic log data are absent. Model velocities are smooth, in the range of ~3400–4250 m/s, and of similar gradient to the starting model (Figure 5c). The model velocity below ~220 m is coincident with the lower range of the highly variable sonic log (Figure 5c). The neutron porosity log shows a decrease from ~50% to ~15% at a depth of ~250 m, suggesting a change in the character of the volcanic rocks.

Well d-96-E (Figure 5g) intersected ~44 m of volcanic rocks of the Ootsa Lake Group, which overlie Cretaceous

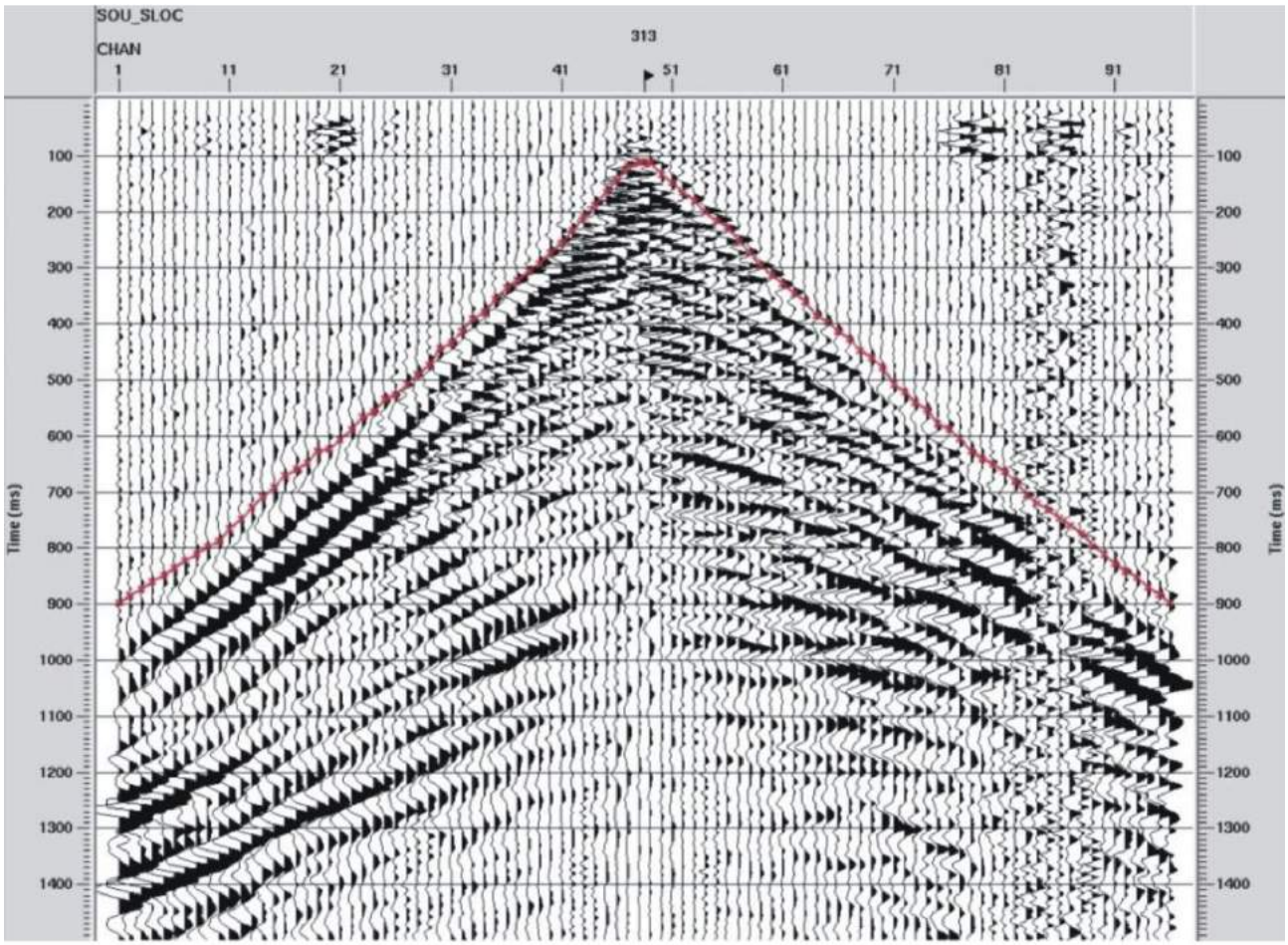

Figure 7: Example of first-arrival traveltime picks of a shot gather from the Canadian Hunter seismic reflection data, southeastern Nechako Basin, south-central British Columbia.

sandstone and conglomerate. Velocity model CH161-03 (Figure 13d) underestimates the velocity above a depth of 150 m. However, immediately to the southwest of the well, constrained by a zone of high ray density (Figure 13c), the model velocity (~3750 m/s) more tightly matches the sonic log (Figure 5g). Maximum ray density occurs at a depth of ~300 m (Figure 5g), where there is a transition from conglomerate above to sandstone below. Below 300 m, the model velocity estimates (~3750–4000 m/s) are within the range of the sonic log.

A Cretaceous conglomerate overlies conglomerate and shale at well a-4-L (Figure 5h) and near-surface volcanic rocks are absent. Rays converge just below the base of the Cretaceous conglomerate at a depth of ~310 m (Figures 5h and 13d). Here, the model velocity (~4000 m/s) shows close agreement with the sonic log. Near-surface sonic data are absent for the overlying sedimentary rocks, but velocities in the adjacent well d-96-E (Figure 5g) are generally below 4000 m/s.

Near-surface volcanic rocks are also absent in well d-94-G (Figure 5e), which intersected a fairly homogeneous sequence of interbedded sandstone, shale and conglomerate of Cretaceous age (Ferri and Riddell, 2006; Riddell et al., 2007). Model velocity (Figure 13f) ranges from ~3500 to ~4000 m/s and, although shallow sonic data are not able to confirm the result, the velocity model echoes the overall trend of the deeper sonic data. The top ~80 m of the well intersected sandstone similar to nearby surface exposures, but the rocks below are generally more fine grained (Ferri and Riddell, 2006). This lithological variation and near-surface weathering may account for the change in gradient of the model velocity in the upper section of the well.

Seismic Velocity Constraint from Well Sonic Logs and Samples

Interpretation of the tomographic velocity models is aided by laboratory samples and borehole sonic logs. The P-wave velocity was measured (G. Andrews, pers. comm., 2009) for approximately 50 samples from the Chilcotin Group, collected primarily within and to the east of the block A area (Figure 4b). Basaltic lava-flow samples from the Chilcotin Group gave a wide velocity range (~4500–6000 m/s), with the majority of values at ~5000–5700 m/s. Anomalously

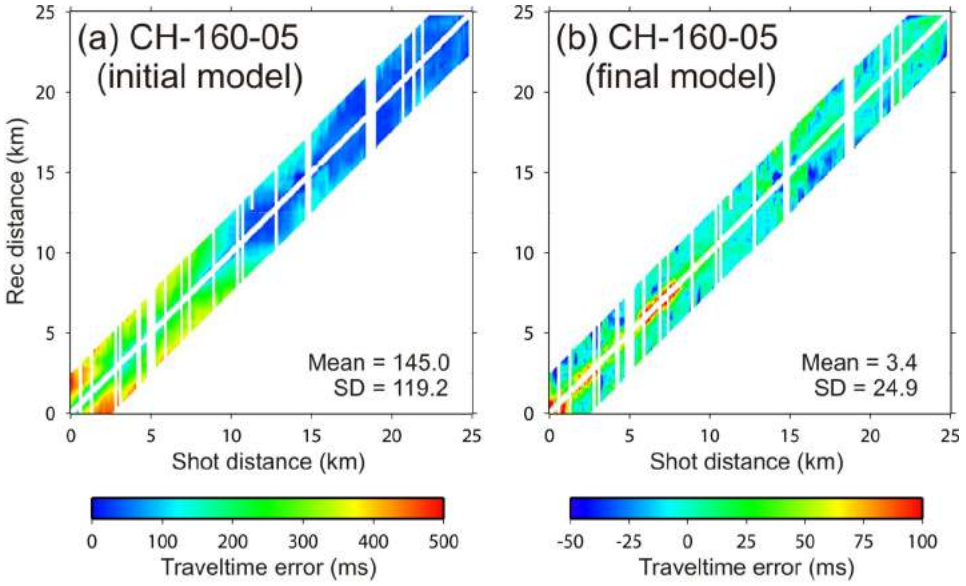

Figure 8. Stacking chart of traveltime errors for line CH160-05, southeastern Nechako Basin, south-central British Columbia: **a)** initial model, **b)** final model. Distances are in kilometres from the north-eastern end of the line.

low velocities of ~4250–4760 m/s were obtained from a sample of volcanic breccia from the Bull Canyon lithofacies, just south of block C. Similarly, three samples from the Chasm lithofacies, to the east of block A, also gave low velocities of ~4070–4710 m/s. One sample of granodiorite from the Jurassic Thuya batholith, to the east of block A, gave high velocities of ~5520–5930 m/s.

A comparison of velocity from models, laboratory samples and well sonic logs is presented in Figure 14. Laboratory samples and sonic logs suggest typical velocities greater

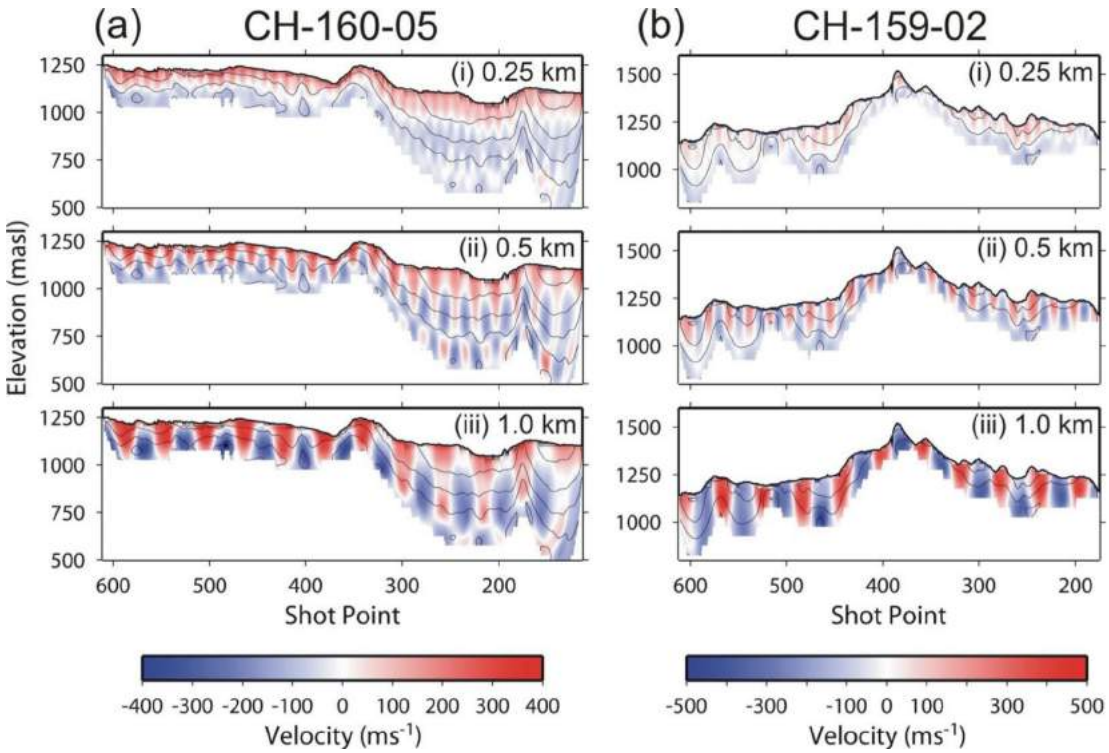

Figure 9. Corrugation models for lines CH-160-05 **(a)** and CH-159-02 **(b)**, southeastern Nechako Basin, south-central British Columbia. Vertical perturbations of slowness of ±10% velocity variation with widths of **i)** 0.25 km, **ii)** 0.5 km, and **iii)** 1 km. Black lines show tomographic velocity contours at an interval of 400 m/s.

Table 1: Thickness of volcanic rocks of the Neogene Chilcotin and Eocene Endako and Ootsa Lake groups intersected by wells in the Nechako Basin, south-central British Columbia (Ferri and Riddell, 2006; Riddell et al., 2007).

Well	Thickness of Volcanic Rocks (m)	Assigned Facies at Surface
Redstone b-82-C	221	Endako Group
Nazko b-16-J	517	Endako Group
Nazko d-96-E	44	Endako Group
Chilcotin b-22-K	116	Chilcotin Group
	477	Ootsa Lake Group?
Redstone d-94-G	0	n/a
Nazko a-4-L	0	n/a

than 4500 m/s for the Chilcotin Group volcanic rocks. Rocks of the Eocene Endako and Ootsa Lake groups exhibit a wide range of sonic log velocities, but most are ~3500–5000 m/s, commonly lower than the Chilcotin Group. Volcaniclastic and sedimentary rocks of Eocene age often show a lower velocity; for example, the shale, siltstone and minor volcanic rocks below the Chilcotin Group in well b-22-K (>120 m) have velocities of ~2900–3500 m/s. This lithological variation within the Eocene Endako and Ootsa Lake groups, with interbeds of lavas that are sometimes vesicular (high porosity), volcaniclastic and sedimentary rocks, and near-surface weathering may explain the wide range of sonic velocities. In seismic reflection surveys of volcanic flows on the Columbia Plateau (Jarchow et al., 1994), interbedding is associated with large contrasts in impedance, which significantly degraded seismic imaging. Similar interbedding of the varied rock types within the Endako and Ootsa Lake groups may also be a reason for the poor seismic imaging associated with some of these rocks.

Model Velocity of the Near- Surface

In order to investigate regional variation in near-surface velocity (in relation to lithology), the mean velocity was calculated from 0 to 175 m (below ground surface) for each velocity model profile. When plotted in map view (Figure 15) along seismic profiles, lateral changes in the mean velocity can be correlated with near-surface geology (Riddell, 2006). The choice of a greater depth range results in data gaps due to locally shallow ray penetration (especially for lines CH159-02 and -02A) and does not alter the overall interpretation. Model velocities for the mapped near-surface rock types are compared with sonic logs and available laboratory samples in Figure 14.

Jura-Cretaceous granodiorite shows the highest velocity for rock types sampled by the models (~3600–4800 m/s), but this is lower than for laboratory samples of the Jurassic Thuya batholith (~5520–5930 m/s). The Cretaceous Spences Bridge Group volcanic rocks similarly have fairly

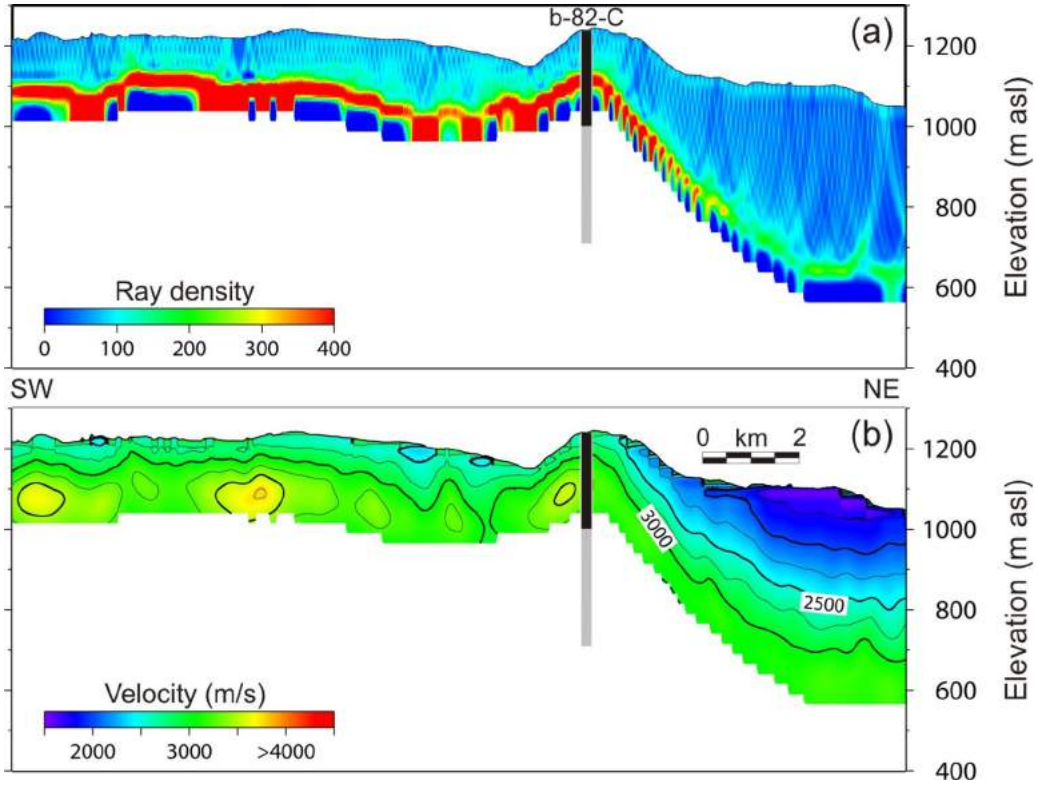

Figure 10: First-arrival tomographic inversion model for Canadian Hunter line CH160-05 (see Figure 4b for location), southeastern Nechako Basin, south-central British Columbia, showing **a)** ray density, and **b)** velocity. Heavy black line shows the thickness of Eocene Endako Group volcanic rocks in well b-82-C (see Figure 5a).

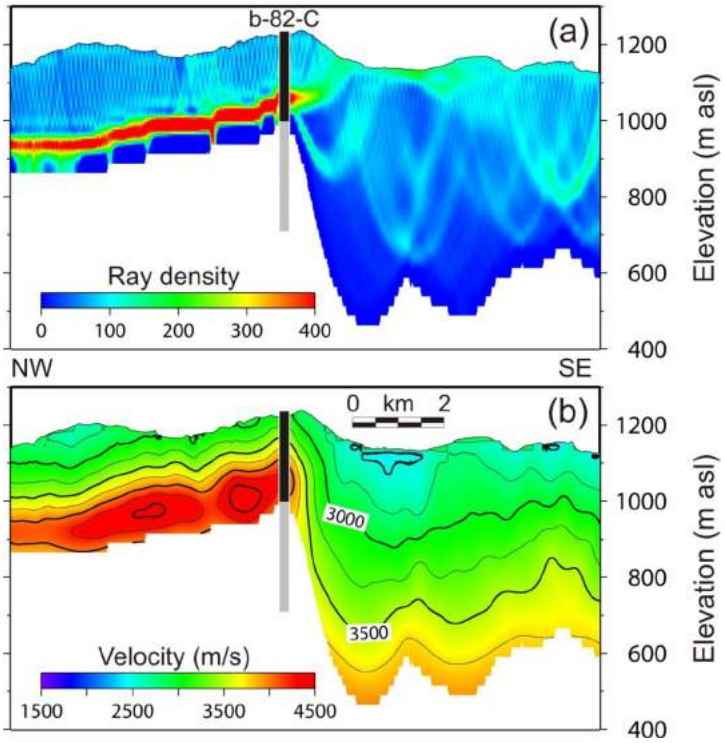

Figure 11: First-arrival tomographic inversion model for Canadian Hunter line CH160-08 (see Figure 4b for location), southeastern Nechako Basin, south-central British Columbia, showing **a)** ray density, and **b)** velocity. Heavy black line shows the thickness of Eocene Endako Group volcanic rocks in well b-82-C (see Figure 5b).

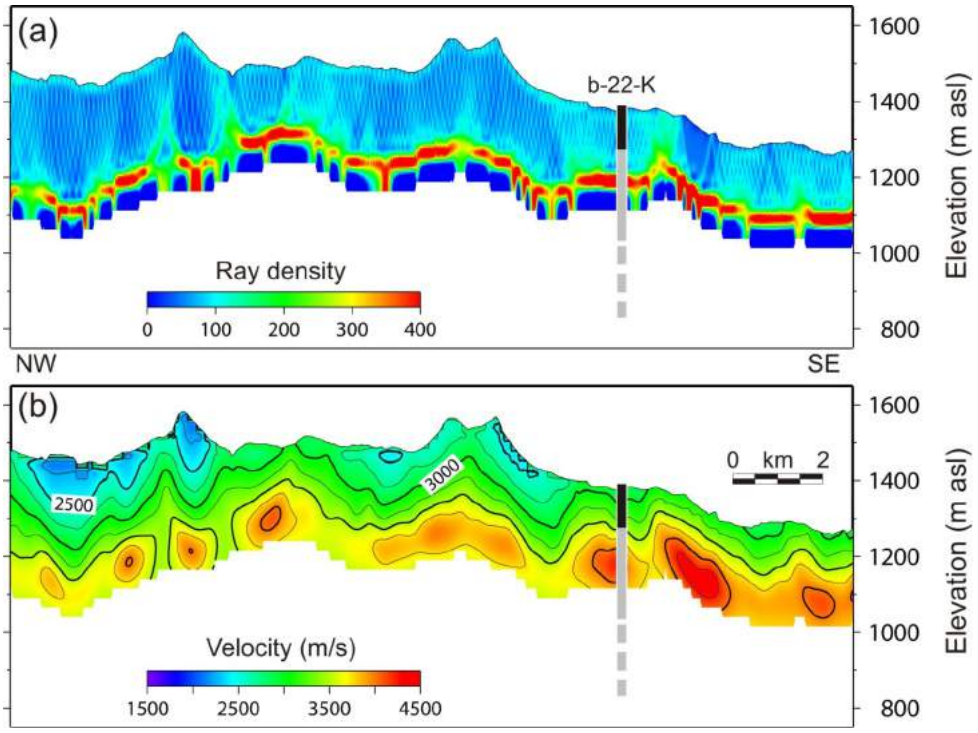

Figure 12: First-arrival tomographic inversion model for a section of Canadian Hunter line CH161-03 (see Figure 4b for location), southeastern Nechako Basin, south-central British Columbia, showing **a)** ray density, and **b)** velocity. Heavy black line shows the thickness of Neogene Chilcotin Group volcanic rocks in well b-22-K (see Figure 5f).

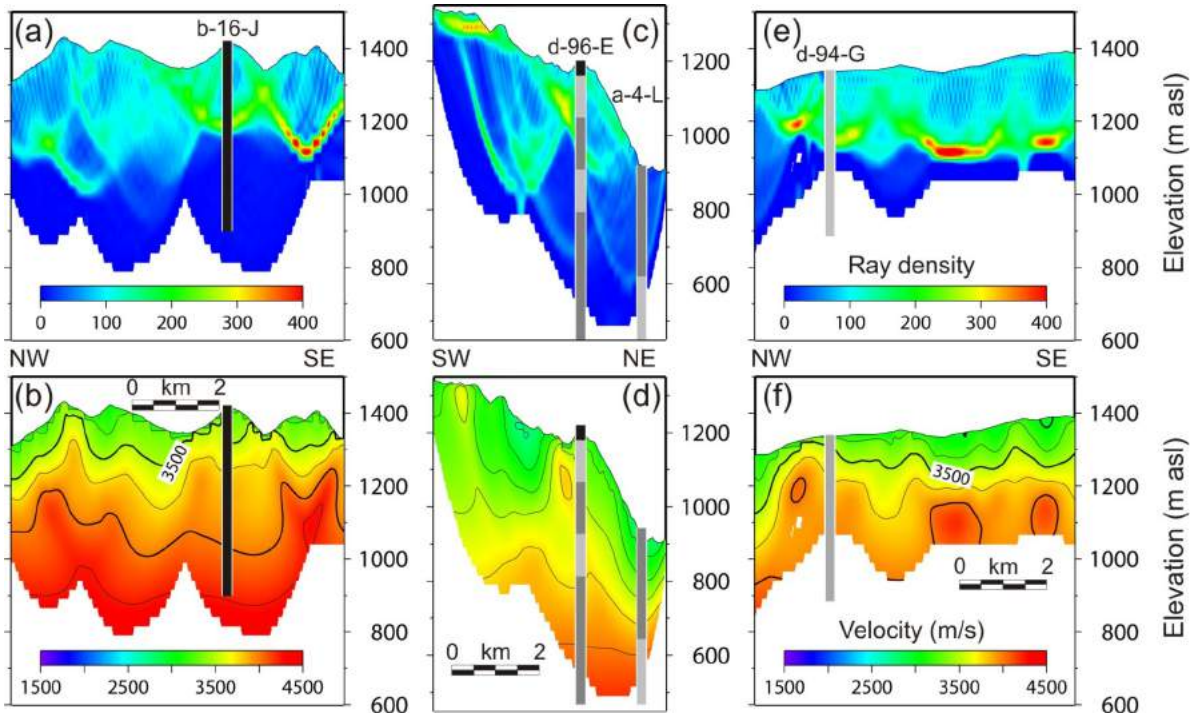

Figure 13: First-arrival tomographic inversion models (see Figure 4b for locations), showing ray density and velocity for sections of seismic reflection lines, southeastern Nechako Basin, south-central British Columbia: **a)** and **b)** line CH-159-09; heavy black line shows the Eocene Endako Group rocks in well b-16-J (see Figure 5c); **c)** and **d)** line CH-159-05; heavy black line shows the Eocene Ootsa Lake Group rocks at the top of well d-96-E and heavy grey lines show changes in the Cretaceous sedimentary rocks of wells d-96-E and a-4-L from finer grained (i.e., shale and siltstone, indicated by darker grey) to coarser grained (i.e., sandstone and conglomerate, indicated by lighter grey; see Figures 5g, h); **e)** and **f)** line CH-160-16; heavy grey line shows well d-94-G (see Figure 5e).

high model velocities (~3400–4200 m/s). The Cretaceous sedimentary rocks have a model velocity range of ~2600–4600 m/s, similar to the sonic logs. The Eocene Endako and Ootsa Lake groups have a model velocity range of ~2600–4600 m/s, which is also in agreement with sonic logs. Although the Endako and Ootsa Lake groups in blocks C and D have a smaller velocity range (3200–4000 m/s) than the Endako Group rocks in block A (3000–4200 m/s), the two groups are not distinguishable on the basis of velocity. Chilcotin Group rocks have much lower model velocities (~1600–3200 m/s; Figure 14) than those from laboratory samples (4500–6000 m/s) and well sonic logs (4200–5300 m/s). These model velocities for the Chilcotin Group are also lower than laboratory samples of volcanic breccia of the Bull Canyon facies (~4250–4760 m/s). The Chilcotin Group model velocity is most similar to that of the Quaternary deposits (2000–2800 m/s).

Block A

Mean tomographic velocities in block A (Figure 15) show typical values of ~3400 m/s, with slightly lower velocities usually associated with the outcrop of Chilcotin Group rocks and Quaternary deposits. The lowest mean velocities in the southeastern Nechako Basin are to the northeast of well b-82-C, where they are commonly ~1900–2400 m/s but can be as low as ~1700 m/s in some locations. These lows correspond to the outcrop of Chilcotin Group volcanic rocks and Quaternary deposits. The changes in ray character in models that cross this zone, specifically lines CH160-05 (Figure 10a), CH160-03 and -02 (Figure 4b), suggest a change in subsurface physical properties. Rays vary from focused convergence at a shallow depth (~200 m) at the margins to a deeper (~450 m) and lower ray density within. Another anomalous low in mean velocity (~2100–2500 m/s) is observed directly to the south of well b-82-C at latitude 51.75°N, longitude 123.25°W (Figure 15).

The outcrop of Spences Bridge Group volcanic rocks and Jurassic or Cretaceous granodiorite north of well d-94-G (Figure 15) is associated with a mean velocity high of ~4200 m/s. High mean velocities (~4300 m/s) towards the centre of line CH-160-04, east of well d-94-G (Figure 15), may be related to the local outcrop of Endako Group volcanic rocks. High values are not, however, observed in association with Endako Group rocks to the south of well b-82-C. The outcrop of Cretaceous sedimentary rocks to the west of well d-94-G also shows mean velocities (~3400–3900 m/s) that are slightly higher than normal.

Ray density and depth predicted by the velocity models are related to the P-wave velocity of the subsurface and the

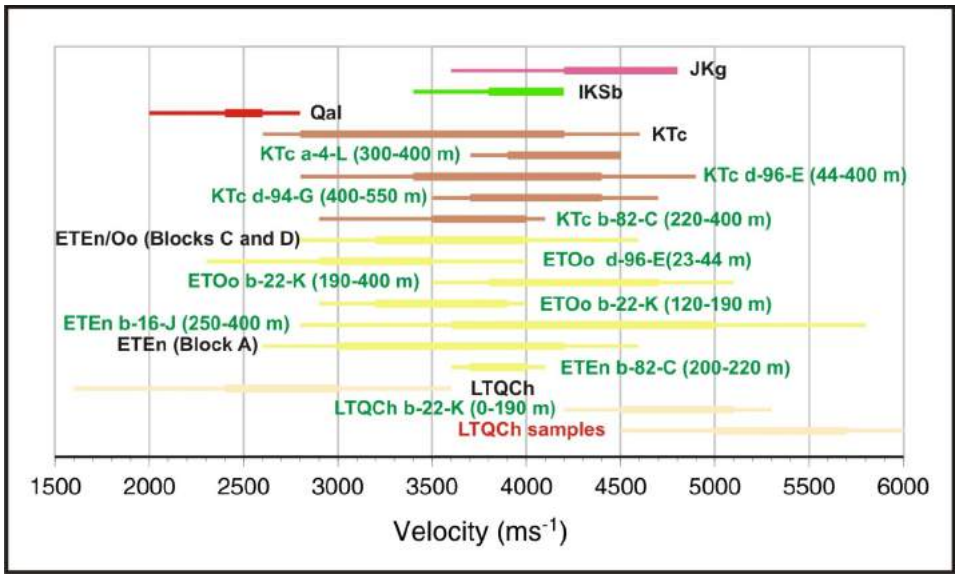

Figure 14: Comparison of seismic velocity from tomographic inversion models (black labels), well sonic logs (green labels) and laboratory samples (red labels) for key rock types in the southeastern Nechako Basin, south-central British Columbia. Thick lines indicate the range of the majority of values. Line colours: pink, Jura-Cretaceous granodiorite; green, Cretaceous Spences Bridge Group volcanic rocks; red, Quaternary deposits; brown, Cretaceous Taylor Creek Group sedimentary rocks; yellow, volcanic rocks of the Eocene Endako and Ootsa Lake groups; beige, Neogene Chilcotin Group rocks.

maximum offset of the seismic reflection profile. The maximum offset used in the Canadian Hunter seismic reflection survey is quite small (2550 m), which places limits on the depth of ray convergence. As a result, for example, rays across most of block A converge at a depth of ~200 m. A high density of rays of this character is observed on models CH160-05 (Figure 10a) and CH160-08 (Figure 11a), at and to the west of well b-82-C, where ~221 m of Endako Group volcanic rocks were intercepted. Rays of similar character can be mapped across the central region of block A to define two areas (orange dashed lines in Figure 15). Outside these areas, rays are less focused and show deeper but variable penetration depths; examples include the southeastern end of CH160-08 (Figure 11a), northeastern end of CH160-05 (Figure 10a) and near well d-94-G (e.g., CH160-16, Figure 13e). This variation in ray character suggests that a change in lithology accompanies a change in subsurface seismic velocity.

Block C

Mean velocities in block C have background values of ~3400 m/s. High mean velocities (up to ~4200 m/s) are generally coincident with the outcrop of Eocene volcanic rocks (Figure 15). The outcrop of Chilcotin Group volcanic rocks and Quaternary deposits, which are observed mainly towards the northwest, are related to lower velocities (down to ~2300 m/s). The predicted bedrock geology (Figure 16), derived from stream sediment geochemistry (Barnett and Williams, 2009), suggests that the Quaternary overburden in this area is underlain by rocks of the Chilcotin Group. The generally poor correlation of mean velocity with the predicted bedrock geology suggests that the near-surface structure and the thickness of the overlying Quaternary deposits have a large influence on the mean velocity. Lithological variation is also suspected to have a large influence. For example, the predicted bedrock geology (Figure 16) reveals that rocks mapped (Riddell, 2006) as the Eocene Ootsa Lake Group have two different geochemical signatures in central block C and northeast of block D, the latter being locally more similar to the Endako Group.

An outcrop of Quaternary deposits in the southeastern corner of block C is also associated with a notably lower velocity (~2300 m/s). A Jura-Cretaceous granodiorite in southern block C (Figure 15) is associated with an anomalously high mean velocity. The width of the velocity anomaly (~4 km) suggests that the intrusion may only be slightly wider in the near surface than its mapped extent beneath the surrounding Quaternary deposits.

A highly variable ray character is observed in block C. Rays exhibit clear focusing along line CH161-03 (Figure 12a), in a region where well b-22-K showed Chilcotin Group basalt overlying shale and siltstone. Within the Jura-Cretaceous granodiorite and also in association with Endako Group rocks to the southeast of well b-22-K, rays exhibit very shallow focusing (~75–175 m and ~75–200 m, respectively). Elsewhere a consistent connection between surface lithology and ray character is not clear, which suggests wide lithological variation. The great thickness of Eocene volcaniclastic deposits, breccia and lava flows (possibly Ootsa Lake Group; Riddell et al., 2007) intersected by well b-22-K suggests that Eocene rocks here have a different

and likely more variable character than the Endako Group rocks in block A.

Block D

Mean velocities in block D (Figure 15) are generally higher, due primarily to the high velocity of volcanic rocks of the Eocene Endako Group (~3700–4000 m/s) and slightly lower velocity rocks of the Ootsa Lake Group (~3100–3900 m/s). The Chilcotin Group in the area around line CH-159-02A (Figures 4b and 15) has velocities higher (~3500–3900 m/s) than typically observed elsewhere in models of the southeastern Nechako Basin. These higher velocities suggest that a thin Chilcotin Group is underlain by the Eocene volcanic rocks.

The Cretaceous sedimentary rocks show two mean velocity signatures. From northern to central block D (lat. 52.6°–52.7°N), the mean velocities (~3400–3600 m/s) are slightly lower than those near well d-94-G (block A). The southernmost outcrops of Cretaceous rocks in block D (lat. 52.55°N, long. 123.4°W) show anomalous lows (~2700 m/s). Surface Cretaceous rocks here were observed to be highly de-

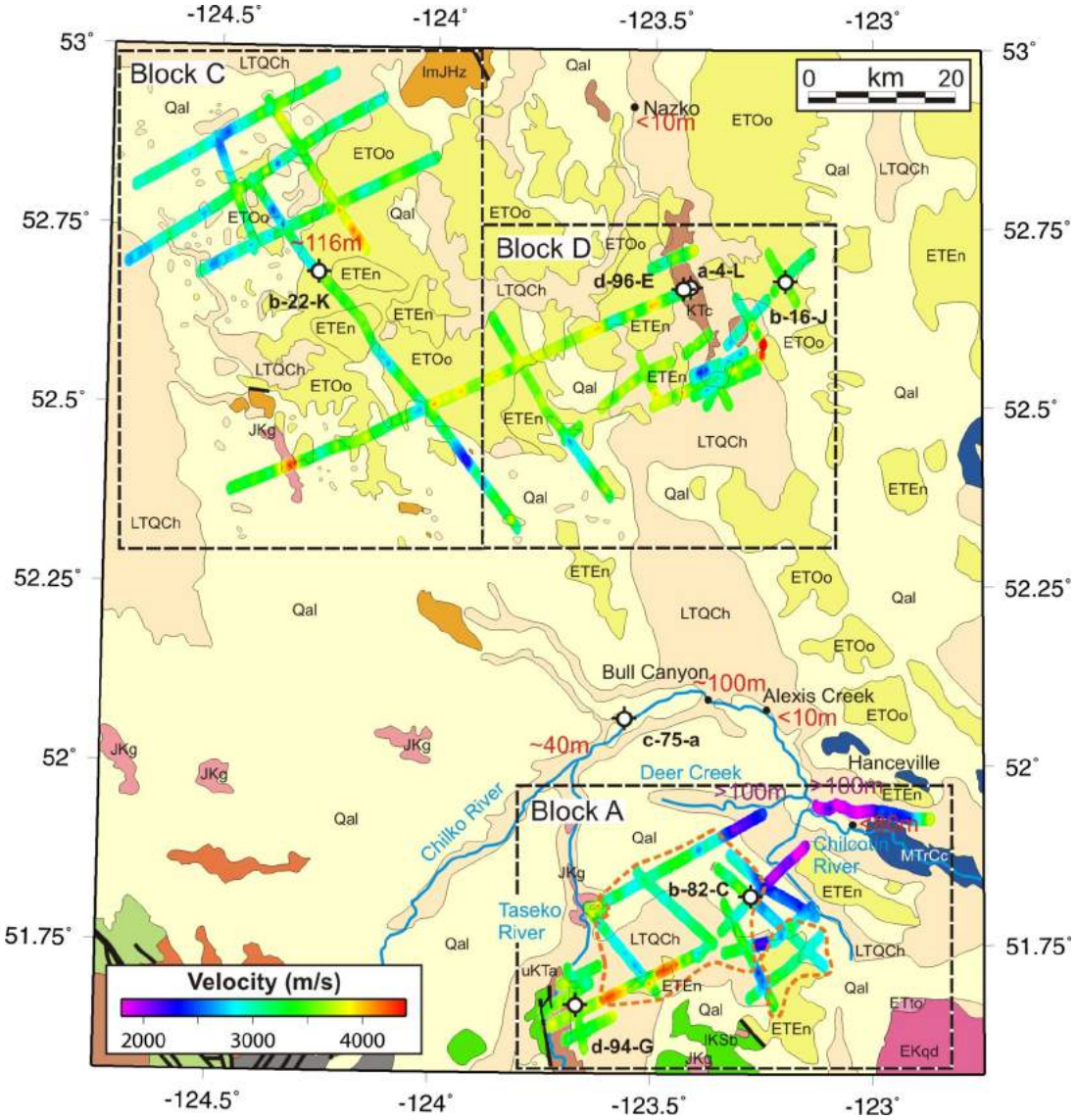

Figure 15: Mean velocity from the ground surface to a depth of 175 m from first-arrival tomographic models, southeastern Nechako Basin, south-central British Columbia. Geological map simplified from Riddell (2006). Red numbers show Chilcotin Group thickness from field and well observations (Andrews and Russell, 2007, 2008; Gordee et al., 2007; Riddell et al., 2007). Purple numbers show the thickness of the Chilcotin Group (Mihalynuk, 2007) modelled from digital elevation models. Orange dashed line shows the probable extent of Eocene volcanic rocks. Blue lines show selected rivers. Heavy dashed black boxes show the study blocks. Abbreviations: ETEn, Eocene Endako Group; ETOo, Eocene Ootsa Lake Group; ETto, Eocene tonalite; LTQCh, Neogene Chilcotin Group; KTc, Cretaceous Taylor Creek Group; EKqd, Cretaceous quartz diorite; uKTa, Taseko River strata; lKSb, Cretaceous Spences Bridge Group; Qal, Quaternary deposits; lmJHz, Jurassic Hazleton Group; JKg, Jura-Cretaceous granodiorite.

formed with near-vertical dips (J. Riddell, pers. comm., 2007). This deformation is related to steep faulting observed on seismic reflection images, and fracture porosity associated with this faulting may account for the lower mean velocity.

In the southwestern corner of block D (CH159-10, Figure 4b), another velocity low (~2800 m/s) is associated with Quaternary deposits (Figure 15) directly to the east of another velocity low in southeastern block C (CH161-03, Figure 4b). Where associated with the Eocene volcanic rocks, rays along line CH159-10 are focused and continuous, similar to those near well b-22-K (Figure 12a). The rays become less dense and penetrate to a greater depth in relation to the outcrop of Quaternary deposits before becoming focused again at the southeast end, where Eocene rocks are again encountered.

Bouguer Gravity of the Southeastern Nechako Basin

Composite Bouguer Gravity Map

New high-resolution airborne helicopter gravity data (corrected with Bouguer densities of 2.30 and 2.67 g/cm^3), acquired by the Geological Survey of Canada in 2008 (Dumont, 2008), provides coverage for the northeastern part of the study region (Figure 17a). Land-based gravity data acquired by Canadian Hunter were used to provide gravity coverage to the southwest. The Canadian Hunter data were manually de-spiked and simple Bouguer corrections applied to the original Bouguer gravity (2.35 g/cm^3). The Canadian Hunter data were low-pass filtered (2625 m-0% to 5250 m-100%), similar to that previously applied to the airborne data.

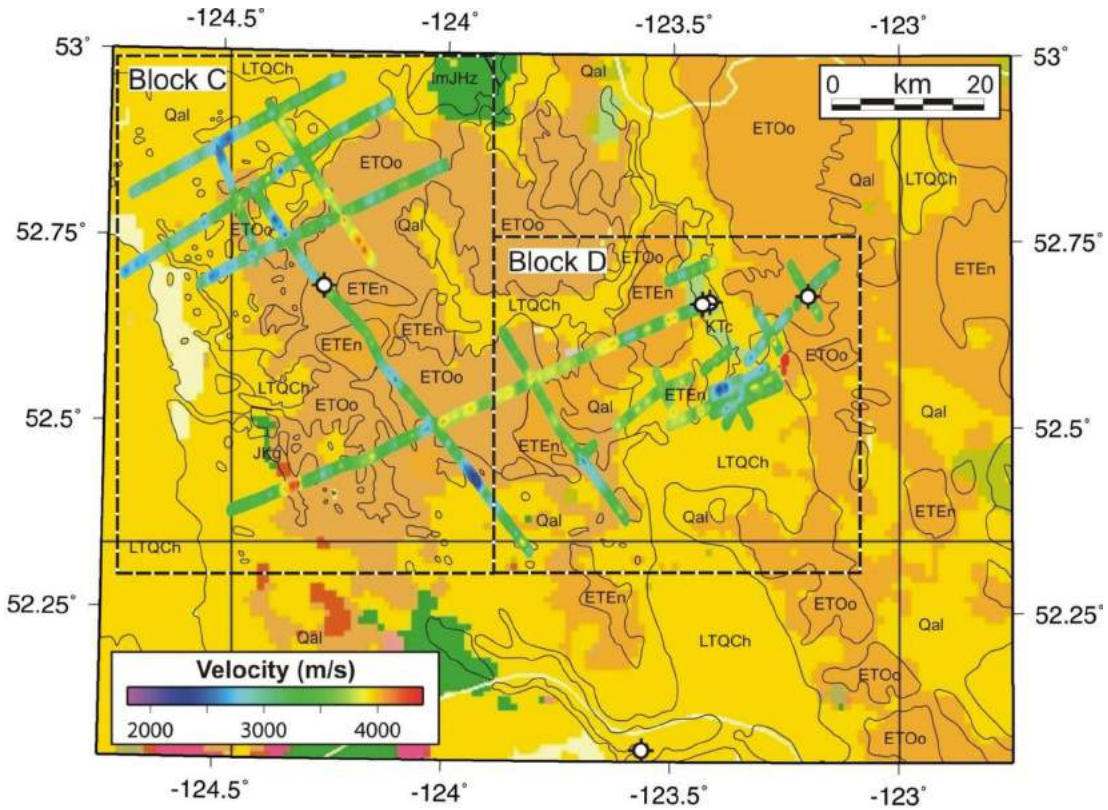

Figure 16: Mean seismic velocity (0–175 m) overlain on the geology predicted from the analysis of stream sediment geochemistry (Barnett and Williams, 2009), southeastern Nechako Basin, south-central British Columbia. Thin black lines and black labels show the geology from the corresponding bedrock geology map (Riddell, 2006). Abbreviations: ETEn, Eocene Endako Group; ETOo, Eocene Ootsa Lake Group; LTQCh, Neogene Chilcotin Group; KTc, Cretaceous Taylor Creek Group; Qal, Quaternary deposits; ImJHz, Jurassic Hazleton Group; JKg, Jura-Cretaceous granodiorite.

The offset of the corrected Canadian Hunter survey from the airborne data is 785.31 mGal (standard deviation 1.52) for a Bouguer density of 2.30 g/cm^3 and 785.82 mGal (standard deviation 1.49) for a Bouguer density of 2.67 g/cm^3. The Canadian Hunter data were levelled accordingly to create the maps shown in Figures 17b and c.

Addition of the sparsely sampled regional land-based gravity data, acquired by the Geological Survey of Canada, resulted in artifacts. These artifacts were point-location gravity highs and lows resulting from a mismatch with the other two surveys. The regional gravity data were therefore omitted in the construction of the final gravity maps.

Preliminary Interpretation of Bouguer Gravity and Velocity Models

First-order comparison of velocity models and Bouguer gravity reveals that there are few relationships between the observed gravity and velocity anomalies. This suggests that the majority of the gravity anomalies are the result of lithological/density variations at depths greater than the penetration of the velocity models. Thus, the mismatch between the mean velocity and gravity anomalies may be indicative of regions where the near-surface geology does not represent the geology at depth.

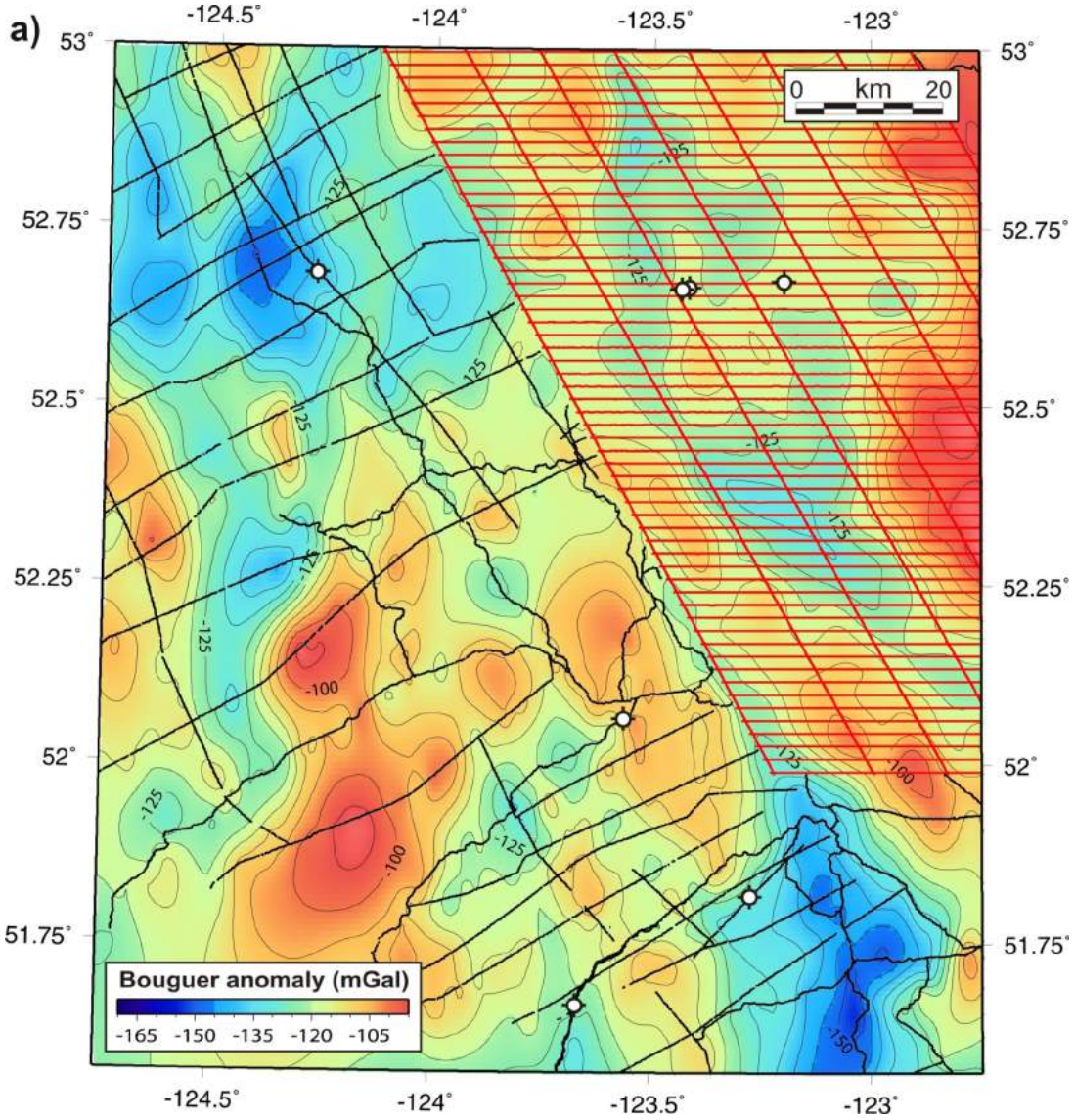

Figure 17. Composite (Canadian Hunter land and Geological Survey of Canada [GSC] airborne data) Bouguer gravity of the southeastern Nechako Basin, south-central British Columbia: **a)** data location; red lines, GSC airborne data; black lines, Canadian Hunter land data; **b) [facing page]** mean velocity (0–175 m) superimposed on the composite Bouguer gravity map corrected to 2.30 g/cm^3; contour interval 5 mGal; **c) [page 222]** mean velocity (0–175 m) superimposed on the composite Bouguer gravity map corrected to 2.67 g/cm^3; contour interval 5 mGal.

However, a number of near-surface velocity anomalies are associated with short-wavelength gravity anomalies. High-velocity anomalies related to Jura-Cretaceous granodiorite and Spences Bridge Group volcanic rocks in northwestern block A (Figure 17) correspond to a small gravity high that likely delineates the extent of these intrusive and/or volcanic rocks. An outcrop of Jura-Cretaceous granodiorite in southern block C exhibits a clear correlation between the high velocity and gravity anomalies, confirming that this intrusion is confined to a small area despite the masking effect of the recent deposits.

Preliminary 3-D Tomographic Velocity Modelling

First arrivals follow the shortest traveltime path from source to receiver, which may not be coincident with the surface trace of the crooked seismic lines. Therefore, a 3-D modelling approach must be applied to estimate near-surface velocity. Crooked seismic lines, which were not modelled by the 2-D methods presented above, include Canadian Hunter lines CH159-01, -01A, 160-01, -18, -19, 161-09 and 162-02, and new Geoscience BC lines 5, 6, 10, 11, 12, 13, and 15 (Figure 18). See Calvert et al. (2009) for detailed information on the acquisition of the Geoscience BC data. The Geoscience BC lines have a greater maximum offset (14 390 m), which will allow the estimation of velocity to a depth greater than for the relatively short offset (2550 m) Canadian Hunter lines.

In order to assess the application of 3-D modelling to crooked lines from the Canadian Hunter survey, and in preparation for analysis of the new data from Geoscience BC, a model was created for (straight) seismic reflection line CH160-05 using the FAST software package (Zelt and Barton, 1998). Model parameters similar to those used for

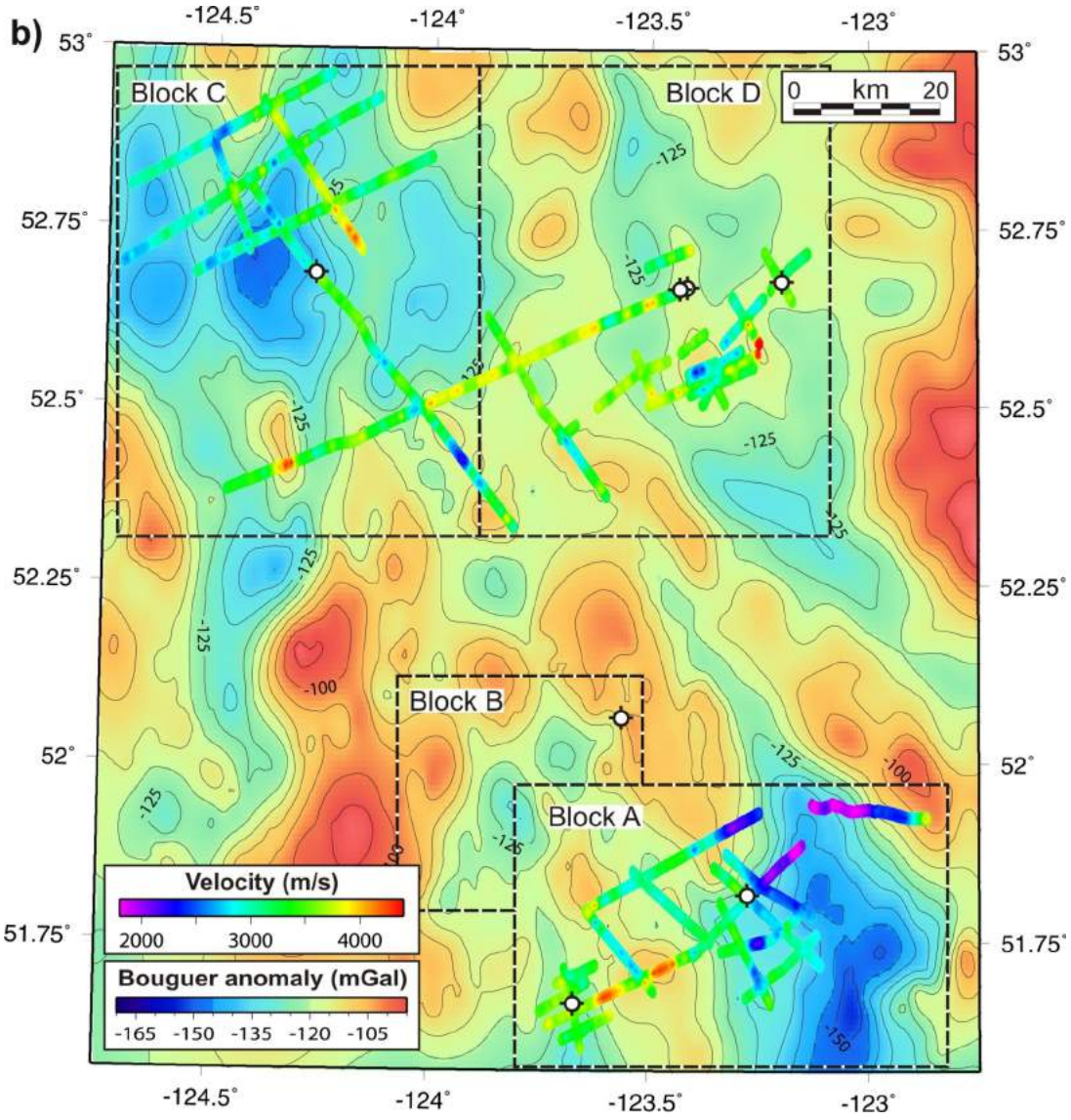

2-D modelling were employed, with a cell size of 25 m and a starting model with a surface velocity of 3500 m/s (gradient of 1.5 s^{-1}). The greatly increased number of cells in a 3-D model can be prohibitive due to a lack of computer memory or extended run time. The northeast-trending seismic line was therefore rotated into an easterly direction to minimize model size.

A perturbation in the velocity model was calculated from the difference between the calculated and observed first-arrival traveltimes for each of nine iterations to give a final velocity model (Figure 19). The models show a reduction in traveltime misfit from an RMS residual of 185.17 ms to 108.11 ms. The velocity and ray data were smoothed for display using a continuous-curvature gridding algorithm (Smith and Wessel, 1990) at a grid spacing of 5 m.

Initial testing of line CH160-05 produces features similar to those of the 2-D model (Figure 19), such as low velocities to the northeast. Following this successful test, the first-arrival traveltimes for Canadian Hunter lines CH159-01, -01A, CH160-01, -18, -19 and CH162-02 were manually edited in preparation for 3-D modelling.

Discussion

Where seismic imaging is poor and outcrop is often obscured by Quaternary deposits and vegetation, tomographic velocity models provide an additional tool in the investigation of the near-surface character of the rocks in the southeastern Nechako Basin. Velocity estimates for most of the primary rock types are in agreement with the velocities obtained from well sonic logs and laboratory samples. However, model velocities from the Chilcotin Group are

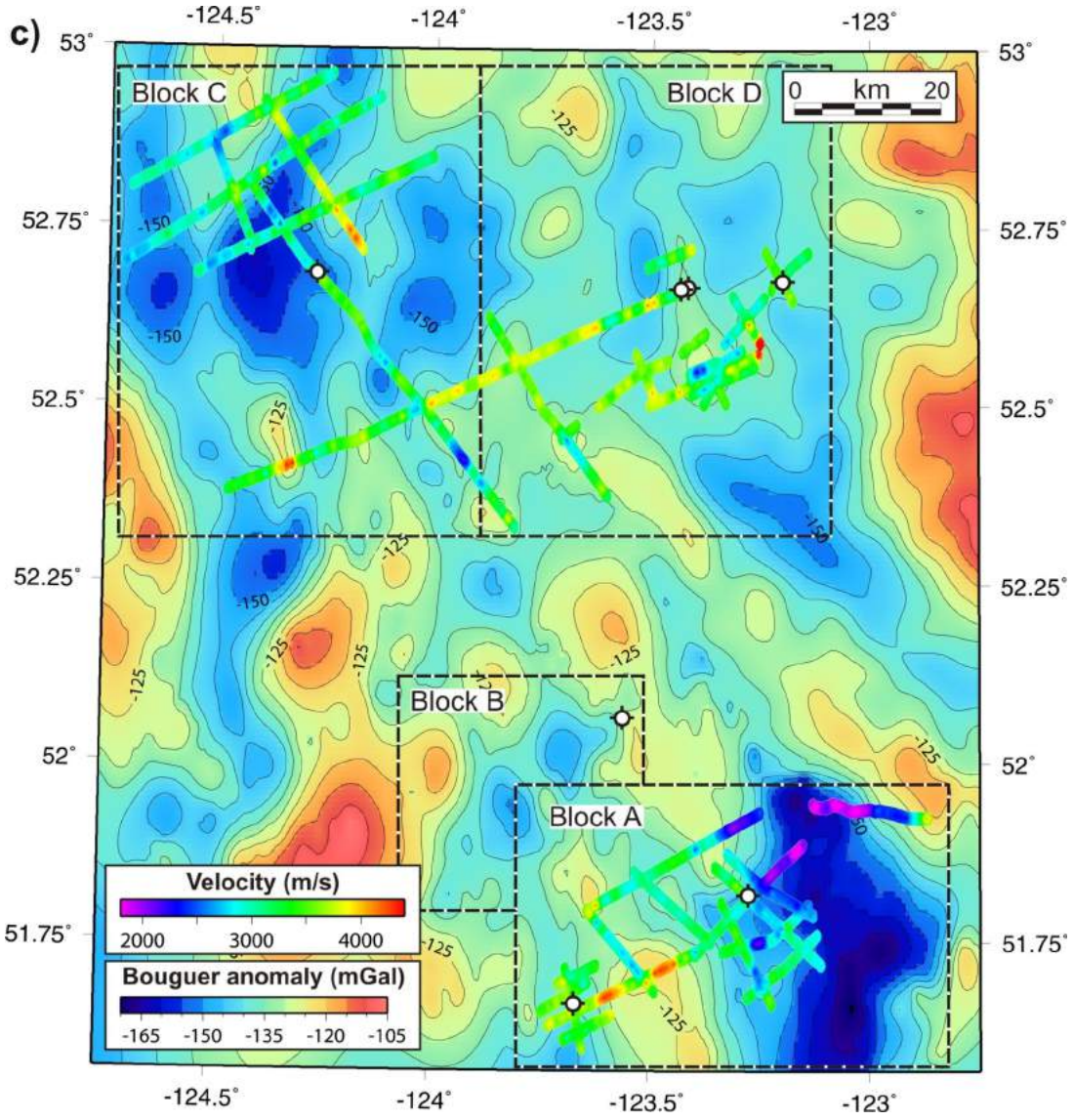

lower than those obtained from laboratory samples and sonic logs, which suggests that the Chilcotin Group is typically of higher velocity than the Eocene Endako and Ootsa Lake groups (Figure 14). The overall model velocity of the Chilcotin Group is similar to that of the Quaternary deposits (2000–2800 m/s).

The Chilcotin Group comprises a number of facies (Andrews and Russell, 2007). The Bull Canyon facies comprises hyaloclastite and breccia, with pillow lavas at the top. These rocks were observed along the Chilcotin River on Highway 20, west of Williams Lake, where it is more breccia dominant (Andrews and Russell, 2007) than at Bull

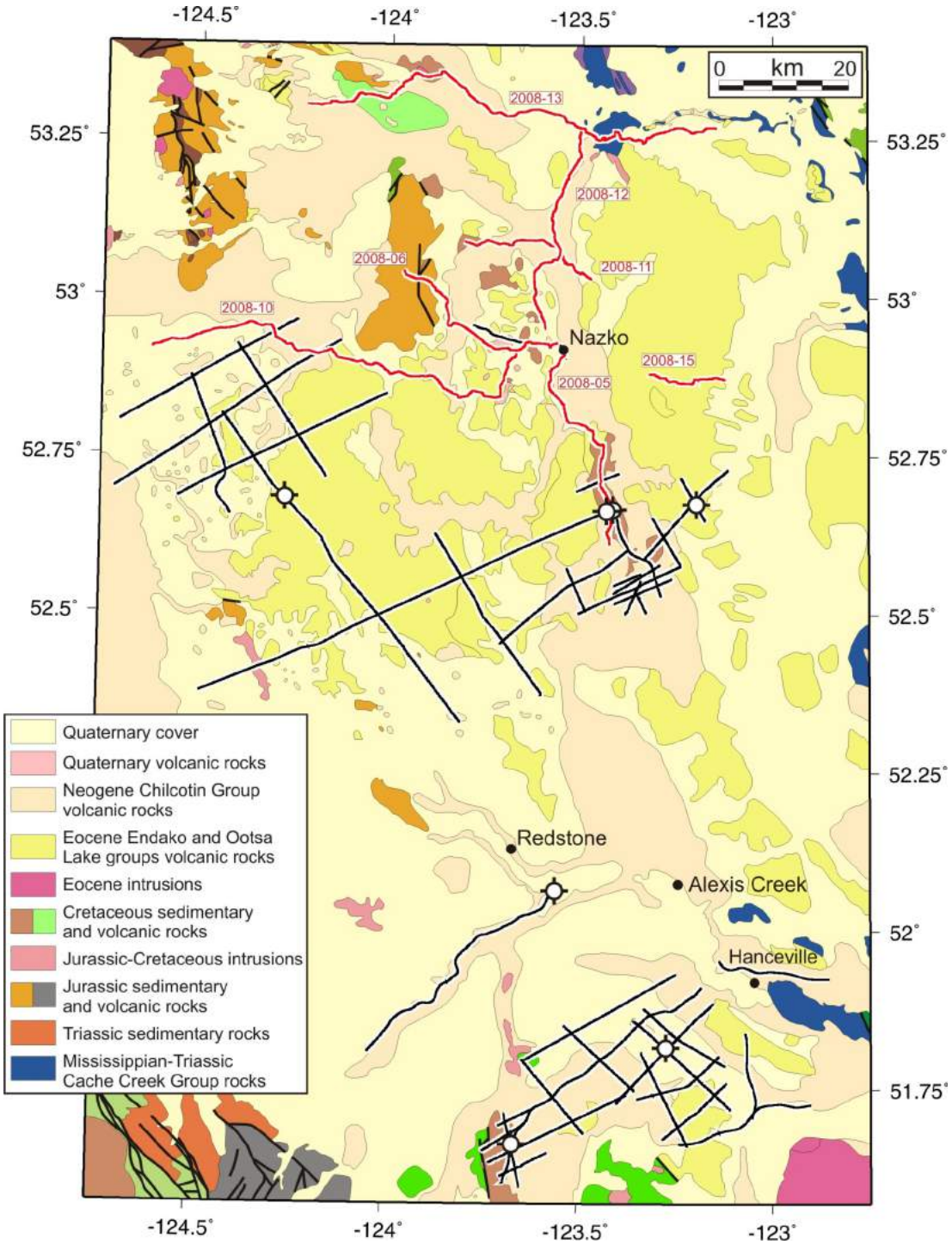

Figure 18: Location of new Geoscience BC vibroseis seismic reflection lines (see Calvert et al., 2009), southeastern Nechako Basin, south-central British Columbia. Red lines show the Geoscience BC data; black lines show the Canadian Hunter data. Bedrock geology modified from Riddell (2006).

Canyon Provincial Park (Figure 15) to the northwest. The Chasm facies consists of thick lavas and hyaloclastite breccia (Andrews and Russell, 2007), which is observed along the Chilko and Taseko rivers (Figure 15). The Dog Creek facies is generally more lava dominant and was described along the Fraser River.

Field investigations (Andrews and Russell, 2008), including the analysis of water-well data, have shown that the Chilcotin Group is regionally thin (<50 m, probably <25 m) and that considerable areas are overlain by Quaternary deposits (typically ~10–50 m; Andrews and Russell, 2008) with variable proportions of basalt contained within (G. Andrews, pers. comm., 2009). Water wells near Alexis Creek (Figure 15) show ~10–50 m of Quaternary drift (Andrews and Russell, 2008). Locally, thicker accumulations of the Chilcotin Group are related to paleo–drainage channels (Andrews and Russell, 2008). In the Chilko River canyon, the Chilcotin Group is ~40 m thick (Andrews and Russell, 2007). Based on water-well samples near Nazko and Alexis Creek (Figure 15), the thickness of the group is estimated to be less than 10 m (Andrews and Russell, 2008). At Bull Canyon Provincial Park (Figure 15), the group is interpreted locally to be ~100 m thick (Gordee et al., 2007). To the southeast, along the Chilcotin River near Hanceville (Figure 15), it has a thickness of <80 m (Andrews and Russell, 2007). To the north, in well b-22-K, it maybe as thick as ~116 m (Riddell et al., 2007).

The results of first-order thickness modelling (Mihalynuk, 2007), based on a digital elevation model (DEM) and mapped basal contacts, echo the interpretation of a regionally thin Chilcotin Group with locally thicker accumulations related to paleo drainage. The model predicts a thickness of ~100–150 m near Hanceville on the Chilcotin River, and a similar thickness to the south of Deer Creek (Figure 15).

In the Chilcotin River area (Figure 15), thick accumulations of Chilcotin Group rocks of the breccia-rich Bull Canyon facies, within a paleo valley, are related to the overall lowest model velocities. These breccias exhibit high porosity and poor consolidation, and often lack a matrix (G. Andrews, pers. comm., 2008), characteristics that would result in the lower seismic velocity relative to consolidated lavas. The elevation of fractured and brecciated Chilcotin Group rocks above the water table at this location would also lower the seismic velocity and may, in part, explain the discrepancy with velocities obtained from fluid-saturated laboratory tests.

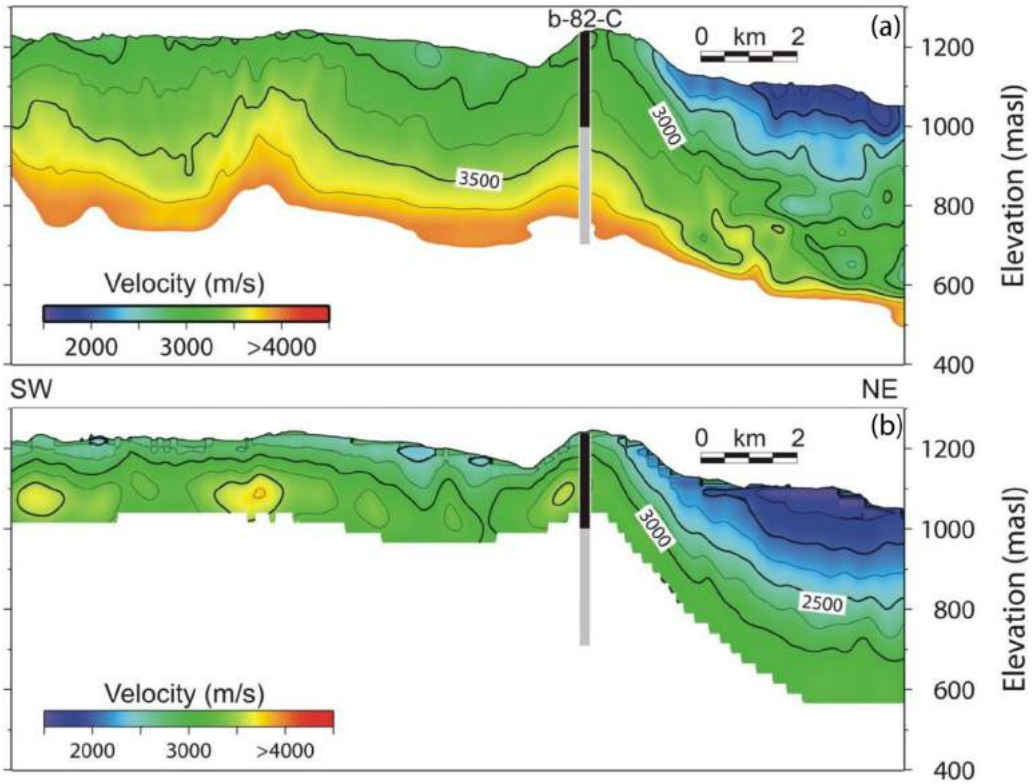

Figure 19: First-arrival tomographic inversion model for Canadian Hunter line CH160-05 (see Figure 4b for location), southeastern Nechako Basin, south-central British Columbia, showing **a)** velocity from 3-D (FAST) model, and **b)** velocity from 2-D (Pronto) model. Heavy black line shows the extent of Eocene Endako Group volcanic rocks in well b-82-C (see Figure 5a).

Anomalously low velocities associated with the Chilcotin Group, such as in northwestern block C and central block A (Figure 15), suggest a mixture of poorly consolidated Quaternary deposits and Chilcotin Group rocks. Elsewhere, the regionally limited thickness of the Chilcotin Group results in the mean velocity being close to that of the underlying rocks.

Ray character (density, focus and penetration depth) and velocity variations were used to define two areas (orange dashed lines, Figure 15) in block A. The tie with well b-82-C (~221 m of Eocene Endako Group) and surface geology allow prediction of the subsurface extent of the Eocene Endako Group in this area. A mean-velocity low to the south of well b-82-C, which divides the two areas, is related to a zone of approximately north-trending strike-slip faulting. Fracturing of rocks in the fault zone, a greater thickness of Quaternary deposits or high-porosity volcanic breccia may account for this velocity low.

Conclusions

Velocity models from the southeastern Nechako Basin agree closely with well sonic logs and laboratory samples. However, mapped occurrences of the Chilcotin Group typically exhibit anomalously low mean velocities, similar to the Quaternary deposits that blanket the region. These low mean velocities likely result from the broad sampling of high porosity, undersaturated, brecciated and fractured rocks, compared to laboratory measurements on water-saturated, consolidated lavas.

In northeastern block A, the lowest mean velocities are related to anomalously thick deposits of the breccia-rich, high-porosity Bull Canyon facies of Chilcotin Group. The distribution of these low mean velocities is consistent with the interpretation of thicker Chilcotin Group rocks in paleo–river valleys.

Where a higher mean velocity is associated with outcrop of the Chilcotin Group, these rocks are locally thin and/or of a velocity similar to underlying rocks. Such Chilcotin Group rocks may be of a more lava-dominant facies, which would have a higher velocity.

The subsurface extent of two areas of Eocene Endako Group, adjacent to well b-82-C, is constrained by variations in the mean velocity and the character (density, focus and penetration depth) of rays, and ties with well and surface geology. These areas are separated by a velocity low related to north-trending strike-slip faulting and possibly a related increased thickness of Quaternary deposits or high-porosity volcanic rocks.

Acknowledgments

The authors thank J. Riddell and F. Ferri for their observations and suggestions regarding the stratigraphic and structural interpretation; and B. Struik for his advice regarding regional tectonics. Funding for this work was provided by Geoscience BC and the Natural Sciences and Engineering Research Council of Canada (NSERC).

References

Aldridge, D.F. and Oldenburg, D.W. (1993): Two dimensional tomographic inversion with finite difference travel times; Journal of Seismic Exploration, v. 2, p. 257–274.

Anderson, R.G., Resnick, J., Russell, J.K., Woodsworth, G.J., Villeneuve, M.E. and Grainger, N.C. (2001): The Cheslatta Lake suite: Miocene mafic, alkaline magmatism in central British Columbia; Canadian Journal of Earth Sciences, v. 38, p. 697–717.

Andrews, G.D.M. and Russell, J.K. (2007): Mineral exploration potential beneath the Chilcotin Group, south-central BC: preliminary insights from volcanic facies analysis; *in* Geological Fieldwork 2006, BC Ministry of Energy, Mines and Petroleum Resources, Paper 2007-1 and Geoscience BC, Report 2007-1, p. 229–238, URL <http://www.em.gov.bc.ca/mining/Geolsurv/Publications/Fieldwork/2006/toc.htm#GeoscienceBC> [November 2009].

Andrews, G.D.M. and Russell, J.K. (2008): Cover thickness across the southern Interior Plateau, British Columbia (NTS 092O, P; 093A, B, C, F): constraints from water-well records; *in* Geoscience BC Summary of Activities 2007, Geoscience BC, Report 2008-1, p. 11–20, URL <http://www.geoscience bc.com/s/SummaryofActivities.asp?ReportID=358405> [November 2009].

Barnett, C.T. and Williams, P.M. (2009): Using geochemistry and neural networks to map geology under glacial cover; Geoscience BC, Report 2009-3, 26 p., URL <http://www.geosciencebc.com/s/2009-03.asp> [November 2009].

Calvert, A.J., Fisher, M.A., Johnson, S.Y. and SHIPS Working Group (2003): Along-strike variations in the shallow seismic velocity structure of the Seattle fault zone: evidence for fault segmentation beneath Puget Sound; Journal of Geophysical Research, v. 108, doi:10.1029/2001JB001703.

Calvert, A.J., Hayward, N., Smithyman, BR. and Takam Takougang, E.M. (2009): Vibroseis survey acquisition in the central Nechako Basin, south-central British Columbia (parts of 093B, C, F, G); *in* Geoscience BC Summary of Activities 2008, Geoscience BC, Report 2009-1, p. 145–150, URL <http://www.geosciencebc.com/s/SummaryofActivities.asp?ReportID=358404> [November 2009].

Dumont, R. (2008): Bouguer anomaly, Nechako Basin airborne gravity survey, Quesnel / Anahim Lake (NTS 93B and part of 93C), British Columbia; Geological Survey of Canada, Open File 5884, 1 map at 1:250 000 scale, URL <http://apps1.gdr.nrcan.gc.ca/mirage/mirage_list_e.php?id=225541> [November 2009].

Farrell, R.E., Andrews, G.D.M., Russell, J.K. and Anderson, R.G. (2007): Chasm and Dog Creek lithofacies, Chilcotin Group basalt, Bonaparte Lake map area, British Columbia; Geological Survey of Canada, Current Research 2007-A5, 11 p., URL <http://geopub.nrcan.gc.ca/moreinfo_e.php?id=223728&_h=Current%20Research%202007-A5> [November 2009].

Ferri, F. and Riddell, J. (2006): The Nechako Basin project: new insights from the southern Nechako Basin; *in* Summary of Activities 2006, BC Ministry of Energy and Mines and Petroleum Resources, p. 89–124, URL <http://www.em

pr.gov.bc.ca/OG/oilandgas/publications/TechnicalDataandReports/Pages/Summary2006.aspx> [November 2009].

Gordee, S.M., Andrews, G.D.M., Simpson, K. and Russell, J.K. (2007): Sub-confined volcanism within the Chilcotin Group, Bull Canyon Provincial Park (NTS 093B/03), south-central British Columbia; *in* Geological Fieldwork 2006, BC Ministry of Energy, Mines and Petroleum Resources, Paper 2007-1 and Geoscience BC, Report 2007-1, p. 285–290, URL <http://www.em.gov.bc.ca/mining/Geolsurv/Publications/Fieldwork/2006/toc.htm#GeoscienceBC> [November 2009].

Grainger, N.C., Villeneuve, M.E., Heaman, L.M. and Anderson, R.G. (2001): New U-Pb and Ar/Ar isotopic age constraints on the timing of Eocene magmatism, Fort Fraser and Nechako River map areas, central British Columbia; Canadian Journal of Earth Sciences, v. 38, p. 679–696.

Hayward, N., and Calvert, A.J. (2007): Seismic reflection and tomographic velocity model constraints on the evolution of the Tofino forearc basin, British Columbia; Geophysical Journal International, v. 168, p. 634–646.

Hayward, N., and Calvert, A.J. (2008a): Structure of the southeastern Nechako Basin, south-central British Columbia (NTS 092N, O; 093B, C): preliminary results of seismic interpretation and first-arrival tomographic modelling; *in* Geoscience BC Summary of Activities 2007, Geoscience BC, Report 2008-1, p. 129–134, URL <http://www.geosciencebc.com/s/SummaryofActivities.asp?ReportID=358405> [November 2009].

Hayward, N. and Calvert, A.J. (2008b): Structure of the southeastern Nechako Basin, British Columbia: interpretation of the Canadian Hunter seismic reflection surveys and preliminary first-arrival tomographic inversion; Geoscience BC, unpublished report.

Hayward, N. and Calvert, A.J. (2009a): Eocene and Neogene volcanic rocks in the southeastern Nechako Basin, British Columbia: interpretation of the Canadian Hunter seismic reflection surveys using first-arrival tomography; Canadian Journal of Earth Sciences, v. 46, p. 707–720.

Hayward, N. and Calvert, A.J. (2009b): Preliminary first-arrival modelling constraints on the character, thickness and distribution of Neogene and Eocene volcanic rocks in the southeastern Nechako Basin, south-central British Columbia (NTS 092N, O, 093B, C); *in* Geoscience BC Summary of Activities 2008, Geoscience BC, Report 2009-1, p. 151–156, URL <http://www.geosciencebc.com/s/SummaryofActivities.asp?ReportID=358404> [November 2009].

Hayward, N., Nedimovic, M., Cleary, M. and Calvert, A.J. (2006): Structural variation along the Devils Mountain fault zone, northwestern Washington; Canadian Journal of Earth Sciences, v. 43, p. 433–446.

Haskin, M.L., Snyder, L.D. and Anderson, R.G. (1998): Tertiary Endako Group volcanic and sedimentary rocks at four sites in the Nechako River and Fort Fraser map areas, central British Columbia; *in* Current Research 1998-A, Geological Survey of Canada, p. 155–164.

Hickson, C.J. (1990): A new frontier geoscience project: Chilcotin-Nechako region, central British Columbia; *in* Current Research, Part F, Geological Survey of Canada, Paper 90-1F, p. 115–120.

Jarchow, C.M., Catching, R.D. and Lutter, W.J. (1994): Large-explosive source, wide recording aperture, seismic profiling on the Columbia Plateau, Washington; Geophysics, v. 59, no. 2, p. 259–271.

Mathews, W.H. (1989): Neogene Chilcotin basalts in south-central British Columbia: geology, ages, and geomorphic history; Canadian Journal of Earth Sciences, v. 26, p. 969–982.

Mihalynuk, M.G. (2007): Neogene and Quaternary Chilcotin Group cover rocks in the Interior Plateau, south-central British Columbia: a preliminary 3-D thickness model; *in* Geological Fieldwork 2006, BC Ministry of Energy, Mines and Petroleum Resources, Paper 2007-1 and Geoscience BC, Report 2007-1, p. 143–147, URL <http://www.empr.gov.bc.ca/Mining/Geoscience/PublicationsCatalogue/Fieldwork/Pages/GeologicalFieldwork2006.aspx> [November 2009].

Price, R.A. (1994): Cordilleran tectonics in the evolution of the Western Canada Sedimentary Basin; Chapter 2. *in* Geological Atlas of the Western Canada Sedimentary Basin, G.D. Mossop, and I. Shetsen (comp.), Canadian Society of Petroleum Geologists and Alberta Research Council, Special Report 4, 510 p., URL <http://www.ags.gov.ab.ca/publications/wcsb_atlas/atlas.html> [November 2009].

Riddell, J.M., compiler (2006): Geology of the southern Nechako Basin, NTS 92N, 92O, 93B, 93C, 93F, 93G; BC Ministry of Energy and Mines and Petroleum Resources, Petroleum Geology Map 2006-1, 3 sheets, 1:400 000 scale.

Riddell, J., Ferri, F., Sweet, A. and O'Sullivan, P. (2007): New geoscience data from the Nechako Basin project; *in* Nechako Initiative Geoscience Update 2007, BC Ministry of Energy and Mines and Petroleum Resources, Petroleum Geology Open File 2007-1, p. 59–98.

Rusmore, M.E. and Woodsworth, G.L. (1991): Coast Plutonic Complex: a mid-Cretaceous contractional orogen; Geology, v. 19, p. 941–944.

Rusmore, M.E., Woodsworth, G.L. and Gehrels, G.E. (2000): Late Cretaceous evolution of the eastern Coast Mountains, Bella Coola, British Columbia; *in* Tectonics of the Coast Mountains, Southeastern Alaska and British Columbia, H.H. Stowell and W.C. McClelland (ed.), Geological Society of America, Special Paper 343, p. 89–105.

Schiarizza, P. and MacIntyre, D.G. (1999): Geology of Babine Lake–Takla Lake area, central British Columbia (93K/11, /12, /13, /14; 93N/3, /4, /5, /6); *in* Geological Fieldwork 1998, BC Ministry of Energy, Mines and Petroleum Resources, Paper 1999-1, p. 33–68.

Schmid, R., Ryberg, T., Ratschbacher, L., Schulze, A., Franz, L., Oberhänsli, R. and Doug, S. (2001): Crustal structure of the eastern Dabie Shan interpreted from deep reflection and shallow tomographic data; Tectonophysics, v. 333, p. 347–359.

Smith, W.H.F. and Wessel, P. (1990): Gridding with continuous curvature splines in tension; Geophysics, v. 55, no. 3, p. 293–305.

Struik, L.C. and MacIntyre, D.G. (2001): Introduction to the special issue of Canadian Journal of Earth Sciences: the Nechako NATMAP Project of the central Canadian Cordillera; Canadian Journal of Earth Sciences, v. 38, p. 485–494.

Zelt, C.A. and Barton, P.J. (1998): 3D seismic refraction tomography: a comparison of two methods applied to data from the Faeroe Basin; Journal of Geophysical Research, v. 103, p. 7187–7210.